Numerical Investigation on Lateral Deflection of Single Pile under Static and Dynamic Loading

Negar Rahemi

Submitted to the
Institute of Graduate Studies and Research
in partial fulfillment of the requirements for the Degree of

Master of Science
in
Civil Engineering

Eastern Mediterranean University
July 2012
Gazimağusa, North Cyprus

Approval of the Institute of Graduate Studies and Research

Prof. Dr. Elvan Yılmaz
Director

I certify that this thesis satisfies the requirements as a thesis for the degree of Master of Science in Civil Engineering.

Asst. Prof. Dr. Murude Çelikağ
Chair, Department of Civil Engineering

We certify that we have read this thesis and that in our opinion it is fully adequate in scope and quality as a thesis for the degree of Master of Science in Civil Engineering.

Asst. Prof. Dr. Huriye Bilsel
Supervisor

Examining Committee

1. Assoc. Prof. Dr. Zalihe Nalbantoğlu

2. Asst. Prof. Dr. Giray Ozay

3. Asst. Prof. Dr. Huriye Bilsel

ABSTRACT

In this thesis a 3D nonlinear analysis was performed to study the lateral deflection of single pile with different slenderness ratios (L/D) under static and dynamic loading. Different models of pile, soil and loading have been simulated, and the lateral deflections were studied considering elastic, elasto-plastic and dynamic models of the soil. For seismic load modeling Ricker wavelet was used. 3D finite element method was applied for numerical modeling and the ABAQUS program version 6.11was utilized to evaluate the lateral deflection of pile.

It was concluded that one of the most effective parameters on lateral deflection of pile is slenderness ratio; the pile length has more influence on increasing the lateral deflection. Furthermore, the lateral deflections versus depth along pile length at the same slenderness ratio revealed that the piles with bigger diameters exhibited less lateral deflections, which might be attributed to the increase in the surface area and hence the skin friction between pile and soil.

Keywords: Finite Element Method, Lateral deflection, Single Pile, Slenderness Ratio, Ricker Wavelet.

ÖZ

Bu tez çalışmasında 3D nonlinear statik ve dinamik analiz yöntemleri ile yanal yükler altında kazık temelin narinlik katsayısının (L/D) yanal deplasmanlara etkisi çalışılmıştır. Farklı kazık, zemin ve yükler modellenmiş ve bunların yanal harekete etkisi irdelenmiştir. Zemin elastik, elastoplastik ve dinamik modellerle simüle edilmiştir. Sismik etkiyi yaratabilmek içinse, sismik modellemede sıklıkla kullanılan ve band-sınırlı bir frekans içeriği olan Ricker dalgacığı kullanılmıştır. 3D modelleme sonlu elemanlar yöntemi ile ABAQUS yazılımı kullanılarak değerlendirilmiştir.

Sonuç olarak yanal deplasmanlar üzerinde en büyük unsurun narinlik katsayısı olduğu ve bu katsayı sabit tutulup kazık boyu ve çapı değiştirildiği zaman, boyunun artmasının yanal deplasmanları artırırken, çapının artmasının ise yanal deplasmanları düşürdüğü gözlemlenmiştir. Ayrıca, çapın artması ile kazık yüzey alanının arttığı ve dolayısıyla sürtünme direncinin de artmasından dolayı yanal deplasmanlarda azalma olduğu sonucuna varılmıştır.

Keywords: Sonlu elemanlar yöntemi, Yanal deplasman, Tek kazık, Narinlik katsayısı, Ricker dalgacığı.

ACKNOWLEDGMENT

I wish to express my gratitude to a number of people who became involved with this thesis. I would like to express my profound appreciation to my supervisor Asst. Prof. Dr. Huriye Bilsel for her continuous caring and valuable guidance in the preparation of this study.

This thesis could not have been accomplished without Nariman, my husband who is always with me, I am indebted to him. He always gives me warm encouragement and love in every situation. He is the center of my universe, and a continuous source of strength, peace and happiness.

I believe I owe deepest thanks to all people in my entire family, my father, my mom and my brother for their patience, love, and continuous presence. Their prayer for me was what sustained me thus far. Words cannot express how grateful I am to them. My deep appreciations also go to my father-in-law and mother-in-law for their unconditional supports and encouragement through all this process. I would like to express my heartfelt gratitude to them.

To the four pillars of my life: God, my husband, and my parents.
Without you, my life would fall apart.

I might not know where the life's road will take me, but walking with You, God, through this journey has given me strength.

Nariman, you are everything for me, without your love and understanding I would not be able to make it.

Mom and Daddy, you have given me so much, thanks for your faith in me, and for teaching me that I should never surrender.

TABLE OF CONTENTS

LIST OF TABLES

LIST OF FIGURES

Chapter 1

INTRODUCTION

1.1 General Observation

Based on recent statistics, many people died in earthquakes worldwide in the last decade. The majority of deaths occurred in developing countries where urbanization and population is increasing rapidly without any serious control. The Middle East region is located at the intersection of main tectonic plates, the African, Arabian and Eurasian plates, cause of very high tectonic activity. Many earthquake disasters in the past happened in the Middle East, influencing most countries in the region. Middle East, extending from Turkey to India is one of the most seismically active regions of world. It is clear that earthquakes not only damage structures and buildings but also influence on human lifeline, social and economic losses. As a result of the high probability of earthquake happening mixed with incremental population, poor construction standards and the absence of correct mitigation strategies, Middle East demonstrates one of the most seismically susceptible regions of the world.

Nowadays, with increasing number of structures and lessening space, the higher and heavier buildings are built by engineers. The costly and strategic structures like skyscrapers, offshore platforms and etc. bring out much important risks and new design problems.

Recent destructive earthquakes in Japan, Turkey, and Iran are reminded the importance of pile foundations and their effect on the response of the supporting structures. The costs of fixing pile foundations are very expensive regarding time and cost. In contrast to shallow foundations, the pile foundations can extend to deeper, stronger soil layers and bedrock to set tolerable resistance. Figure 1 indicated typical pile foundations for different structures.

Although the static loading is necessary in pile designing, it is the dynamic loading which presents the important challenge to the design engineer. Dynamic excitation and lateral loading poses extra forces on the pile foundations. These pile foundations have to be designed to protect lateral loads cause of earthquakes, wind, and any impact loads. It is often essential to do a dynamic analysis of the pile for lateral vibrations, to sufficient representation pile response under earthquake vibrations. Figure 2 demonstrates the general description of the problem follow study (Gazetas & Mylonakis, 1998). It is illustrated in the general case of an embedded foundation supported with piles but all the final results are logical for any foundation type. Descriptions of wave characteristics and particle motions for the four wave types are given in Table 1.

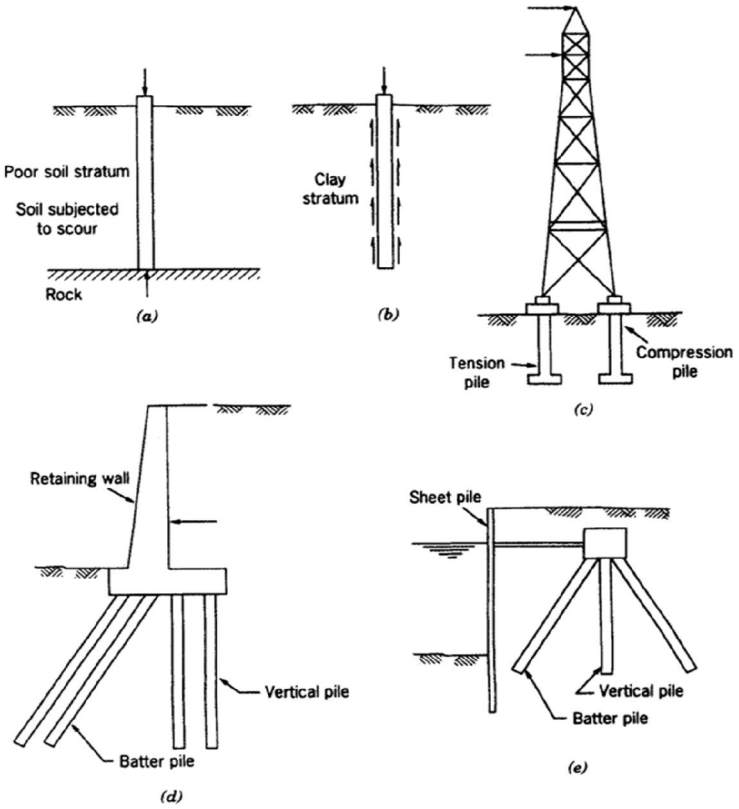

Figure 1: Typical models of pile foundations (a) Bearing pile, (b) Friction pile, (c) piles under uplift, (d) piles under lateral load, (e) Batter piles under lateral load (Prakash & Sharma, 1990)

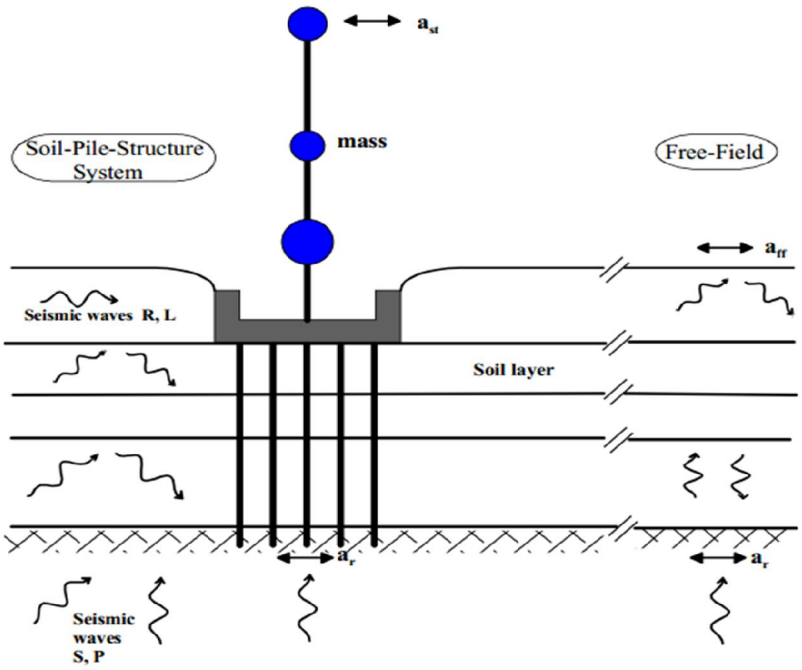

Figure 2: Schematic soil-pile structure interaction under seismic excitation

Table 1: Seismic waves properties (Braile, 2010)

Wave Type (and names)	Particle Motion	Typical Velocity	Other Characteristics
P, **Compressional**, Primary, Longitudinal	Alternating compressions ("pushes") and dilations ("pulls") which are directed in the same direction as the wave is propagating (along the ray path); and therefore, perpendicular to the wavefront.	V_P ~ 5 – 7 km/s in typical Earth's crust; >~ 8 km/s in Earth's mantle and core; ~1.5 km/s in water; ~0.3 km/s in air.	P motion travels fastest in materials, so the P-wave is the first-arriving energy on a seismogram. Generally smaller and higher frequency than the S and Surface-waves. P waves in a liquid or gas are pressure waves, including sound waves.
S, **Shear**, Secondary, Transverse	Alternating transverse motions (perpendicular to the direction of propagation, and the ray path); commonly approximately polarized such that particle motion is in vertical or horizontal planes.	V_S ~ 3 – 4 km/s in typical Earth's crust; >~ 4.5 km/s in Earth's mantle; ~ 2.5-3.0 km/s in (solid) inner core.	S-waves do not travel through fluids, so do not exist in Earth's outer core (inferred to be primarily liquid iron) or in air or water or molten rock (magma). S waves travel slower than P waves in a solid and, therefore, arrive after the P wave.
L, **Love**, Surface waves, Long waves	Transverse horizontal motion, perpendicular to the direction of propagation and generally parallel to the Earth's surface.	V_L ~ 2.0 - 4.4 km/s in the Earth depending on frequency of the propagating wave, and therefore the depth of penetration of the waves. In general, the Love waves travel slightly faster than the Rayleigh waves.	Love waves exist because of the Earth's surface. They are largest at the surface and decrease in amplitude with depth. Love waves are dispersive, that is, the wave velocity is dependent on frequency, generally with low frequencies propagating at higher velocity. Depth of penetration of the Love waves is also dependent on frequency, with lower frequencies penetrating to greater depth.
R, **Rayleigh**, Surface waves, Long waves, Ground roll	Motion is both in the direction of propagation and perpendicular (in a vertical plane), and "phased" so that the motion is generally elliptical – either prograde or retrograde.	V_R ~ 2.0 - 4.2 km/s in the Earth depending on frequency of the propagating wave, and therefore the depth of penetration of the waves.	Rayleigh waves are also dispersive and the amplitudes generally decrease with depth in the Earth. Appearance and particle motion are similar to water waves. Depth of penetration of the Rayleigh waves is also dependent on frequency, with lower frequencies penetrating to greater depth.

The main objective of this investigation is to assess the lateral deformation of pile in sand with elastic behavior and elasto-plastic behavior, under static and dynamic loading with finite element method. Due to the limited goal of this study, the analysis is concentrated on a single pile located in homogenous soil deposit, and evaluated as a semi-infinite space. The pile has a straight axis, circular cross section, and it is placed vertically.

Chapter 2

LITERATURE REVIEW

Chapter 2 reviews the literature on soil-pile interaction under lateral loads. The goal of this chapter is to review past research on pile behavior under static and dynamic loadings in cohesion-less soils. The simulating and modeling of soil-pile interaction and analysis of pile behavior under dynamic and static loads are the two main sections of this study.

2.1 Analytical Models for Static Lateral Loading of Piles

There are three main approaches for evaluating pile deflection under lateral loading, as Poulos and Davis (1980) and Fleming et al. (1992) are illustrated.

2.1.1 Beam on Elastic Foundation Method

In 1867 Winkler proposed this model, which was introduced as Beam on Elastic Foundation (BEF) and Beam on Winkler Foundation (BWF). This model suggests that in soil-pile contact at any point along the pile length, there is a linear relationship between deflection (v) and pressure (p), and the contact stresses at other points are independent.

Additionally, the model represents the soil as a series of unconnected linearly-elastic distributed springs (Ochoa, 2003), as shown in Figure 3. The pile is simulated as a beam-column element.

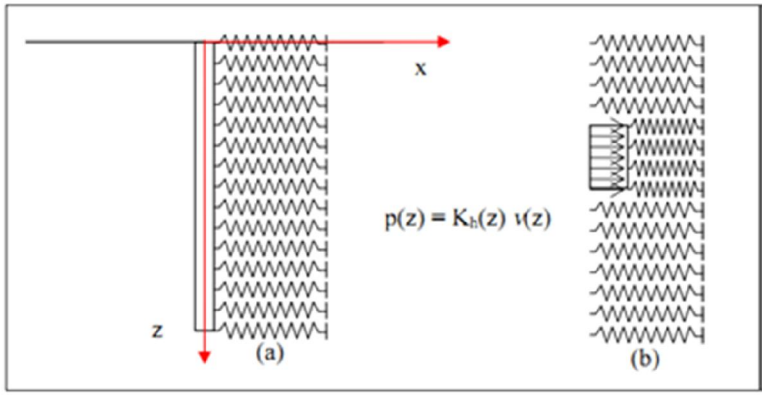

Figure 3: Subgrade Reaction Modulus Model, (a) Soil and Pile reaction, (b) Soil model and the influence of a partial uniform pressure over it (Poulos & Davis, 1980)

K_h (Force/Length^3) is the oil modulus of lateral (horizontal) subgrade reaction, represented by the spring modulus of the model, and is the horizontal pressure needed to create a unit horizontal displacement. K_h depends on foundation size, depth and soil type.

The equation of equilibrium of the beam (pile) under the influence of distributed load (w) is shown in Equation 2.1.

$$E_p I_p \frac{d^4 V}{dZ^4} = -W = -pd = -K_h V d \qquad (2.1)$$

$$E_p I_p \frac{d^4 V}{dZ^4} + K_h V d = 0$$

where:

E_p = pile modulus of elasticity

I_p = pile cross section moment of inertia

d = pile diameter

w = soil reaction per unit length over the pile (distributed load)

p = soil pressure over the pile

K_h = soil lateral subgrade-reaction modulus

V= Lateral displacement of the pile

Analytical solutions, despite the fact that limited concerning practical applications, present a consequential perception in to the pile reaction and the factors which impact the soil-pile interaction. These solutions have been acquired for the Equation 1.1 for the case of constant k_h with specific boundary condition and depth (for example, Hetenyi (1946) and Scott (1981), describes the Hetenyi solution in a detail procedure).

Vesic (1961) obtained accurate elastic solutions of infinite beams on isotropic half space acted upon by couple and concentrated loads. He suggested values for the subgrade reaction modulus by comparing these solutions with the Winkler method solutions. Therefore, the Winkler model provides logically accurate results for the subgrade reaction modulus under medium and long length beams.

Kagawa (1992) assessed the factors affecting the subgrade reaction modulus K_h, and presented one dimensional analysis, suggesting a protocol to obtain an average value of K_h as a function of the Soil Young's Modulus which may be used for pile analysis established upon the BEF.

A logical method of analysis of beam on elastic foundations was improved by Vlasov & Leont'ev (1966) on the basis of the elastic continuum approach; considering only the vertical displacements in the continuum (horizontal displacement were assumed to be zero). Finite Difference Method (FDM) has been recommended and carried out since the early fifties; for instance by Palmer and Thompson (1948), Reese and Matlock (1956).

The basic differential Equation 1, in this model is written in finite-difference form, and the solution is found at separate points. The general separated model for FDM is presented in Figure 4. The discretization of the solution with the FDM has the disadvantages such as the difficulty to define general boundary conditions at the tip and top of the pile, and that the elements have to be uniform in size.

Foundation engineering books like Bowles (1974) and Bowles (1996) can be used as a reference for numerical solutions with the Finite Element Method with one-dimensional elements, or beam elements. This model is mostly mentioned as the Stiffness Method.

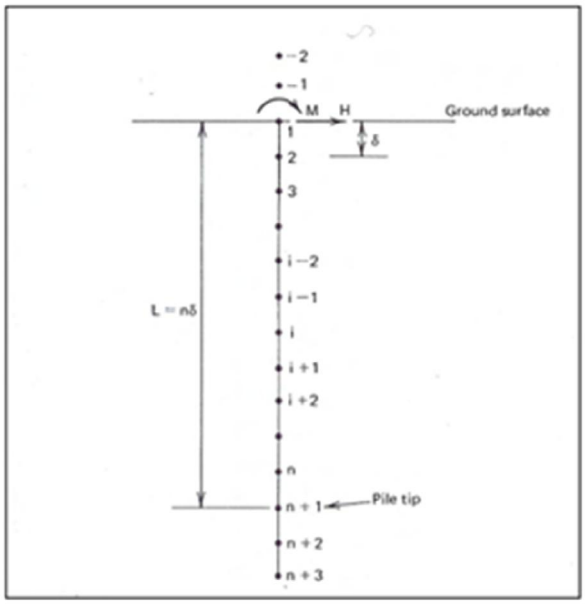

Figure 4: Finite Difference Analysis Model for Laterally Loaded piles (Poulos & Davis, 1980)

Some authors suggest a complete design procedure for piles have been used the Beam on Elastic Foundation method (BEF). Possibly, the most familiar of these approaches is worked by Broms (1964a, 1964b, 1965). For predicting the deflection under working loads, and for estimating ultimate load resistance supplied by

assuming a number of simple ultimate states for the soil-pile system, the BEF method is used.

2.1.1.1 The p-y Method

The original Beam on Elastic Foundation (BEF) model does not explain the non-linear reaction of the soil by itself. P-y method is the most common model to consider the non-linear nature of soil reaction. In this approach the spring stiffness value is variable, allowing consideration of a non-equivalent relationship between the soil resistance per unit pile length (p) and the lateral displacement (y).

Reese and Matlock (1956) and co-workers have improved the p-y method. Various researchers have presented methods of solution by the FDM method and determined the p-y curves for different soils and depths based on experimental results, and obtained information on how to improve a computer program [(Matlock & Reese, 1960), (Matlock, 1970), and (Reese, 1977)]. A schematic of the soil-pile modeling and the p-y curve for each non-linear spring is shown in Figure 5.

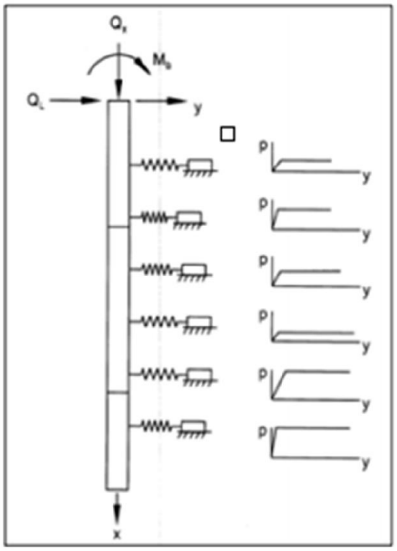

Figure 5: P-y Diagram Model for Soil-Pile (FHWA, 1997)

Figure 6 shows a distribution of contact stresses before and after pile lateral deflection. It is important to mention that (p) is not a contact stress, but the consequent of the contact stresses and friction along the pile perimeter for a specified depth. The (p) value depends on soil type and depth, pile shape and type, and the deflection amount (y) when the reaction is non-linear.

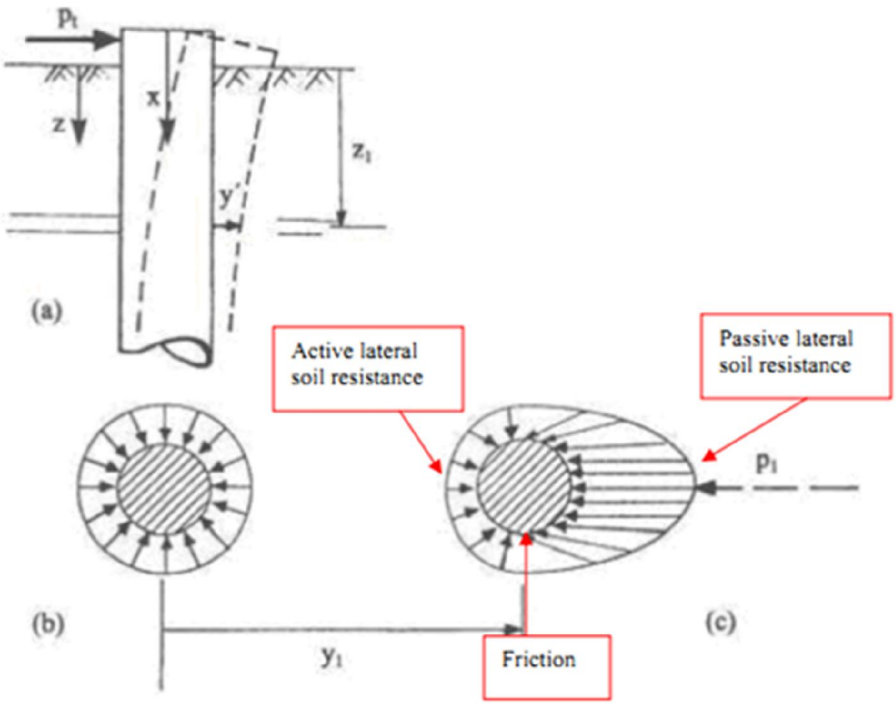

Figure 6: Contact Stresses Distribution against the Pile Before and After Lateral Bending (Reese & Van Impe, 2001)

For various types of soils, different p-y curves have been improved which are demonstrating the magnitude of soil pressure as a function of the pile deflection [(Reese & Welch, 1975), Reese et al. (1974), (Matlock, 1970), (Georgiadis, 1983), Brown et al. (1994), (Bransby M. , 1999), (Ashour & Norris, 2000)].

Sometimes the p-y method is mentioned as the (BNWF) Beam on Non-linear Winkler Foundation system to model the soil-pile interaction such as Wang et al. (1998) and Hutchinson et al. (2004), or as the Load Transfer Method (Basile, 2003).

The p-y method or the finite difference methods in many analyses including the subgrade reaction method were replaced by Finite Element Method, with improvement of this model (Hsiung & Chen, 1997), (Sogge, 1981).

In spite of the fact that the concentration the p-y method is not resulted the ultimate capacity of laterally loaded piles. Nevertheless this method cannot be suitable to determine the ultimate capacity cause of yielding of the soil. To estimate the ultimate capacity due to soil yielding, with the assumption of the soil is perfectly plastic; the Beam on Elastic Foundation method is used.

2.1.1.2 The Wedge Model

The Strain Wedge Method, which lets the evaluation of non-linear p-y curve reaction of laterally loaded piles settled on the three dimensional soil-pile interaction response through a passive wedge soil developing in front of the pile, improved by Ashour et al. (1998), Ashour and Norris (2000) as shown in Figure 7 and Figure 8. It should be noted that the Matlock and Reese (1960) p-y curve was based on the results of field tests on instrumented piles. This method allows relating the stress-strain-strength acting of the layered soil in the 3D wedge approach to the 1D BNWF model parameters. So, the non-linear reaction may be achieved from the analysis that looks at the actual conditions of soil-pile system (soil layers classification, pile diameter, etc.).

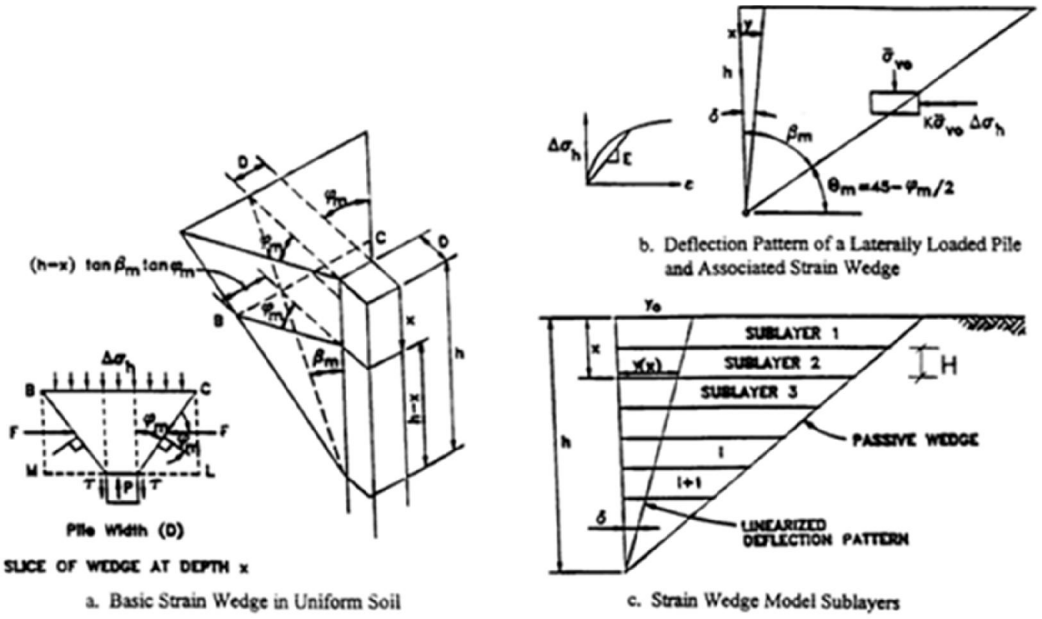

Figure 7: Schematic of Strain Wedge Model for Analyzing Lateral Load Pile (Ashour and Norris, 2000)

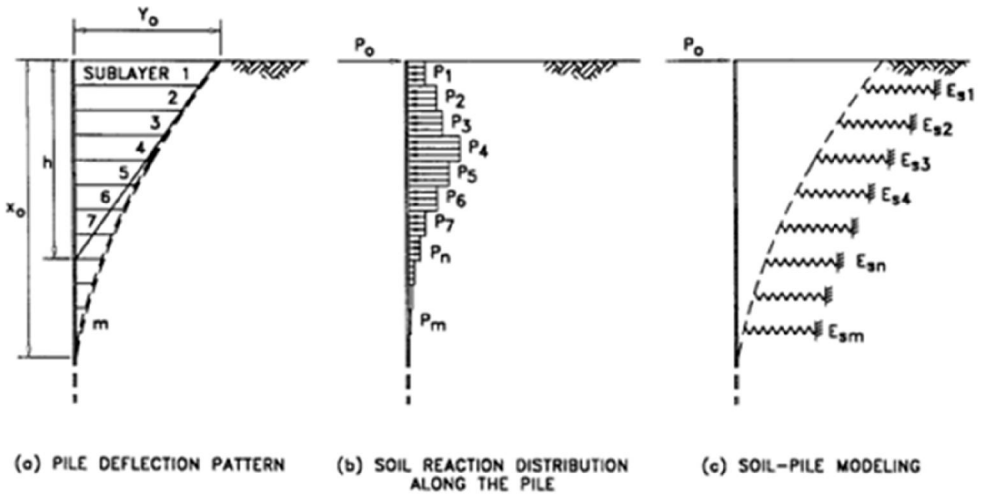

Figure 8: Distribution of Soil-Pile Interaction along Deflected Pile (Ashour and Norris, 2000)

2.1.1.3 New Developments in BEF

The Winkler method to predict soil-pile reaction under static lateral loads is used for BEF analysis which still is a topic of research. Some of the recent developments are considered here. Shen and Teh (2004) recommended a variation method (same as the

Ritz approach) to present the analysis of the laterally loaded pile in a soil with subgrade reaction modulus increasing by depth. For the maximum bending and deflection of laterally loaded piles in a soil with uniform subgrade reaction modulus, (Hsiung, 2003) has proposed the theoretical method. In a site in Korea, Kim et al. (2004) have managed lateral field tests on instrumented piles, acquiring the p-y curves and evaluating the effect of the installation method and fixed head conditions in the soil-pile response.

2.1.2 Elastic Continuum Theory

The modeling of the soil as a homogeneous elastic continuum has been suggested for the analysis of the soil-pile interaction. For the analysis of limit pile capacity, Plane Strain Models were developed with some authors like Davis and Booker (1971). For modeling the 3D system as a series of parallel horizontal planes in plane strain, the Plane Strain Models are used which are related to the case of shallow-embedded sheet piling.

Douglas and Davis (1964); Spillers and Stoll (1964); Poulos (1971, 1972), and other authors developed Three Dimensional Elastic models. These models were established on Mindlin's method for the horizontal displacement due to a horizontal point load within the interior of a semi-infinite elastic-isotropic homogeneous mass which can be found in various Elasticity handbooks, such as Poulos and Davis (1974).

Douglas and Davis (1964); Spillers and Stoll (1964) and Basile (2002) recommended integral solutions over a predefined area, representing a fraction of the pile surface, since Mindlin's solutions become singular when evaluating the displacement corresponding to the point where the load is located. These solutions which define

the displacement field due to an assumed loading system (pattern) associated with the pile-soil interaction, are generally known as Green Functions.

Utilization of the model suggested by Poulos (1971, 1972), was presented by Poulos and Davis (1980) . The pile is assumed to be a thin rectangular vertical strip divided in elements in this model, and it is observed that each element is acted upon by uniform horizontal stresses as it shown in Figure 9 which are related to the element displacements through the integral solution of Mindlin's problem.

At last, in which soil pressures over each element are unknown variables, they realized the differential equation of equilibrium of a beam element on an infinite soil with the Finite Difference Method (FDM). The displacements are found after achieving the pressures.

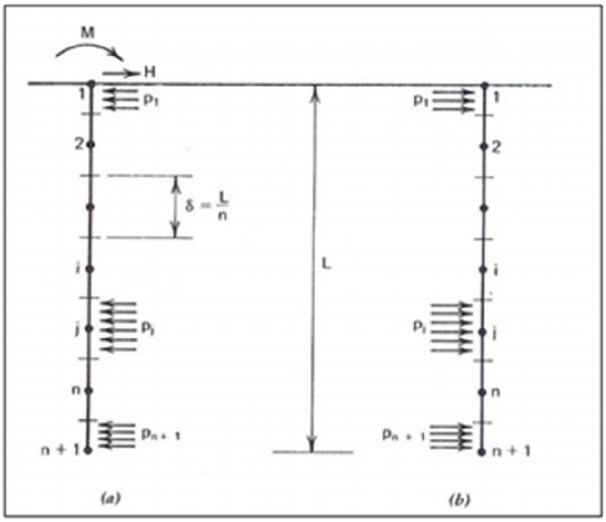

Figure 9: Continuous Analysis Model of Soil-Pile Stress reacting on (a) Pile, (b) Soil around the Pile (Poulos & Davis, 1980)

The ability to take into consideration the homogeneous nature of soil, the semi-infinite dimension of the half-space, and the boundary conditions along the unloaded

ground surface is the advantage of this model. Although yielding of soil may be presented by varying the soil elastic modulus, this method does not allow to consider local yielding and layered soil conditions.

In this way, Spillers and Stoll (1964) suggested the calculation of the maximum allowable load by any appropriate yielding condition (e.g. a wedge model for the top part of the soil, where the yielding of soil happens and displacements are larger), together with the elastic solution and a repetitive procedure to control that the maximum load is not exceeded at any point.

Two of the disadvantages of the discretization by cooperating with means of the FDM is that the difficulty to present general boundary conditions at pile top and bottom, and the needed uniform size of the elements. This soil model was used for the BEM (Boundary Element Method) analysis of piled foundations, as Basile (2002) informed.

2.1.3 The Finite Element Theory

The Finite Element Method (FEM) has been recommended and implemented to perform a numerical analysis of the soil-pile system to obtain solution for laterally loaded flexible piles in an elasto-plastic soil mass.

Poulos and Davis (1980) informed that the first tries included two-dimensional finite element models in the horizontal plane Baguelin and Frank (1979); general 3D finite element analysis recommended by Desai and Appel (1976), and axis-symmetric geometries by Banerjee and Davis (1978).

Some recent work such as Yang and Jeremic (2002) used 3D Finite Element Methods of a laterally loaded pile driven in layered and uniform soil profiles so that numerically achieve p-y curves and compare them to experimental ones as shown in Figure 10.

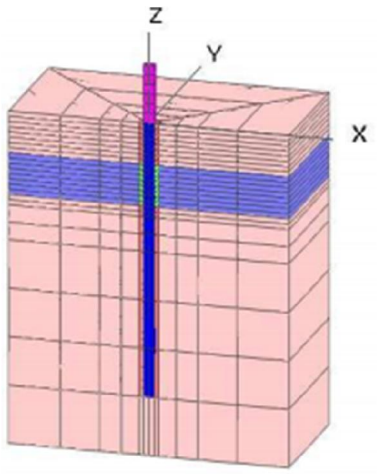

Figure 10: A Model of a 3-Dimensional Finite Element Mesh for a Single Pile (Yang & Jeremic, 2002)

Permitting to account for soil non-linearity by applying appropriate constitutive models like the Drucker-Prager model is the Finite Element Method ability, [(Ben Jamma & Shiojiri, 2000); (Yang & Jeremic, 2002)], and using gap-elements to be able to model soil-pile separation. Capabilities of these modeling are usually available in strong general purpose objective FEM programs such as ABAQUS and ANSYS or limited geotechnical engineering software like PLAXIS.

Mostafa and EI Naggar (2002), Wang et al. (1998), EI Naggar and Novak (1996), Kagawa (1992), and Poulos and Davis (1980) agreed that using FEM analysis is feasible for the design of large structures only. This is due to the cost of the specialized software, the time needed for non-linear analysis, the time required for model creation, the difficulty in explanation of the result in terms of usual pile

(beam) variables, and the un-certainties related with soil non-linear modeling in 3D. Figure 11 presents the finite element meshes utilized for a single micro pile in the numerical analyzing.

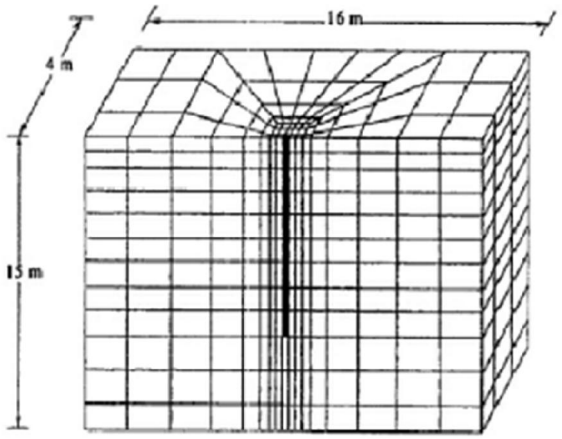

Figure 11: A Model of a 3-Dimensional Finite Element Mesh for a Single Pile after (Shahrour, Ousta, & Sadek, 2001)

Finally, the practical 3D finite difference method program in recent years called Flac3D has been used to analyze the complex geotechnical problems, but for pile analysis it has been rarely used. Ng and Zhang (2001) used 3D finite difference method to evaluate the behavior of piles placed on a cut slope.

They studied the influence of the sleeving (doughnut of compressible stuff which is usually built between the shafts and adjacent soil to reduce the lateral load transfer from the buildings to the shallow depths of the slope) on the pile performance, as shown in Figure 12.

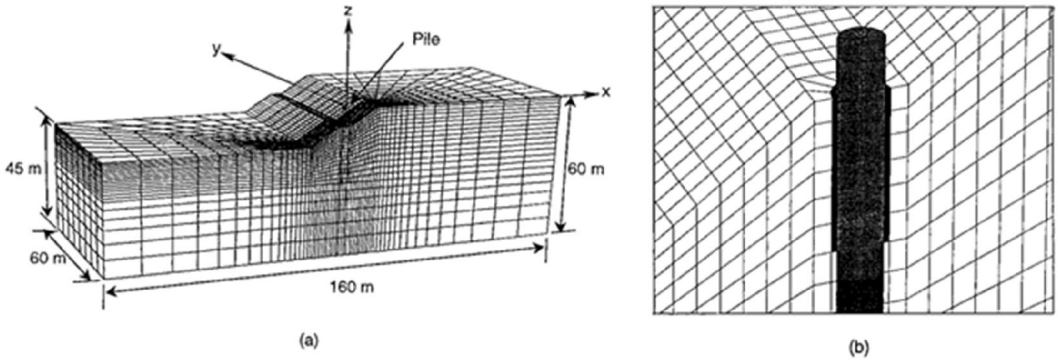

Figure 12: Finite Difference Meshing (a) Three Dimensional View, (b) Zoom in View of Sleeved Region (Ng & Zhang, 2001)

2.2 Analysis of Piles under Dynamic Lateral Loads

In this section, methods of modeling dynamic behavior of single piles under lateral loads such as seismic shock have been presented. These are Beam on Non-linear Winkler Foundation (BNWF), which defines the soil as a series of continuous springs, Continuum Methods, which makes closed form analysis by assuming soil as an infinite semi-space, Boundary Element Method (BEM), and Finite Element Method (FEM), which defines the soil as a homogenous medium. A short explanation of these approaches is discussed in this section, with special mention on seismic analysis.

2.2.1 Continuum Model

Automatically inclusion of radiation of energy to infinity, called Radiation Damping through the complicated explanation of pile stiffness, is the main advantage of the Continuum Method over the FEM and BNWF.

The drawbacks are that, in general, it is only feasible for visco-elastic materials, in spite of that material damping may be considered by using the complicated form of the material properties, or Lame's invariants. Only by changing the elastic modulus of the full space, the non-linear behavior of the soil can be accounted. This is another

disadvantage of the continuum approach. In addition, the soil medium should be homogeneous or consist of homogeneous layers, with confined boundary conditions.

In spite of this method's limitations, it is very useful to obtain a better understanding of the soil-pile interaction, and to acquire the analytical explanation of parameters, like Subgrade Reaction Modulus (Vesic, 1961), which can be utilized in the Winkler Model.

The summary of some studies which are related to the aim of the present research can be summarized as follows:

An approximate continuum model to explain soil-pile interaction proposed by Novak (1974), where the soil is supposed to made up of a set of independent horizontal layers of very tiny thickness, extending to infinity.

This model may be observed as a generalized Winkler Method, due to having an independent plane. The planes are mentioned to be in a plane strain, and those are isotropic, homogeneous, and linearly elastic.

A differential equation of the damped pile in horizontal motion was formulated by Novak (1974). For harmonic vibration persuaded through pile ends, he proposed the Steady State solution, and used it for different boundary conditions to determine dynamic stiffness of the pile head.

The dimensionless variables which control the soil-pile system reaction, according to Novak (1974) are:

(1) The relation between the shear wave velocity of the soil (V_s) and the longitudinal wave velocity of pile (V_c), (wave velocity ratio (V_s/V_c),

(2) The relation between specific mass of the soil (ρ) and the specific mass of the pile (ρ_p), (mass ratio ρ / ρ_p),

(3) The load frequency (ω) (generally as a dimensionless parameter $a_0 = r_0 \omega \times \sqrt{\frac{\rho}{G}}$, where G is the shear modulus of the soil),

(4) The relation between the pile length (L) and the pile radius (r_0), (slenderness ratio L / r_0),

By considering a rigid pile cap at the pile heads for a pile group and single pile head, Novak (1974) recommended the equivalent damping and stiffness constants. He suggested a numerical example, and compared the reaction of a spread footing with pile foundations, obtaining the following results:

(1) Pile foundations natural frequencies and resonant amplitudes are more than spread footings, but their damping are smaller and those are more rigid, (2) The resonant amplitudes can decrease due to pile (and spread footing) embedment, (3) The Dynamic Analysis of pile foundations is more important than shallow foundations because they can't do away with vibrations, however the piles can decrease the settlements.

As Klar (2003) reported, the stiffness acquired from the Novak (1974) solution approaches to zero, as the frequency approaches to zero. Additionally, Novak's methods approach to Tajimi's method (based on a more accurate 3D analysis) by frequency rising. Because higher frequency wave tends to spread more horizontally,

Novak's model predisposes to get the real behavior. Hence, at very low frequencies and static states Novak's solution gives poor results, where for high frequencies it gives better results.

For comparison with the Winkler model (where the soil is designed as separate springs and dashpots), Nogami and Novak (1980) studied the coefficient of dynamic soil response to pile movement, treating the soil as a 3D continuum. They obtained the followed conclusions by these assumptions:

The Assumptions: (a) Cylindrical elastic pile driven to the bedrock; (b) Homogeneous soil layer overlying a rigid bedrock; (c) The soil vertical motion is ignored; (d) Constant hysteretic damping material for linear viscoelastic soil; (e) Harmonic movement; (f) No relation between soil-pile interface and soil-pile movement.

The conclusions: (1) The soil damping and local stiffness strongly varies with frequency, depth, and with respect to soil-pile stiffness; (2) The 3D explanation is the same as 2D plane strain explanation when the frequencies are larger than the basic frequency of the soil layers, as recommended by Novak (1974), and (3) For piles with stiffer materials and soil deposits with greater depth, it is better to use the Winkler assumptions. The outcomes of earlier works were not exactly used to evaluate the soil mass contribution to the dynamic response in a distinct Winkler model. However these can be used in assessing the pile dynamic stiffness (Impedance) and modeling the damping and stiffness influences of the soil-pile dynamic reaction in the Winkler method.

2.2.2 Winkler Model

Since the seventies Matlock et al. (1978) the p-y methods for explaining the lateral stiffness of soil-pile model for seismic analysis has been utilized, taking in to account that both pile and soil can treat in a nonlinear manner during greatest events. Wang et al. (1998), Polam et al. (1998), and Boulanger et al. (2004) have worked on this model. According to p-y model, the cyclic soil degradation should be using. For executing this analysis, the common linear modal analysis should be replaced by an iterative nonlinear time-domain analysis, as the expected nonlinear response cannot be feasible by linear modal analysis Brown et al. (2001).

Material Damping is the energy scattering which is intrinsic material behavior, and can define the soil stiffness by a dashpot in parallel with a spring. This is the famous Kelvin-Voigt model for visco-elastic materials.

Figures 13 and 14 present the hysteretic damping, which is the energy scattering due to soil nonlinear behavior, which can be explained in p-y method by letting the unloading path to differ from loading path Brown et al. (2001).As the cyclic loading proceeds, soil strength decreases which is known as soil degradation.

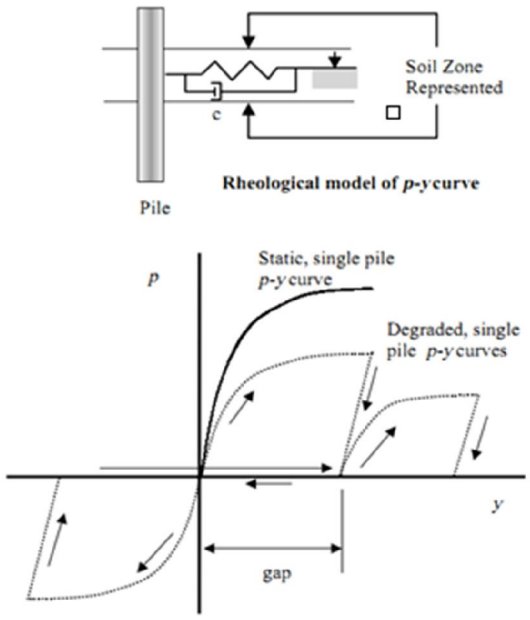

Figure 13: P-y Method for Hysteretic Damping and Cyclic Degradation in Soil (Brown et al., 2001)

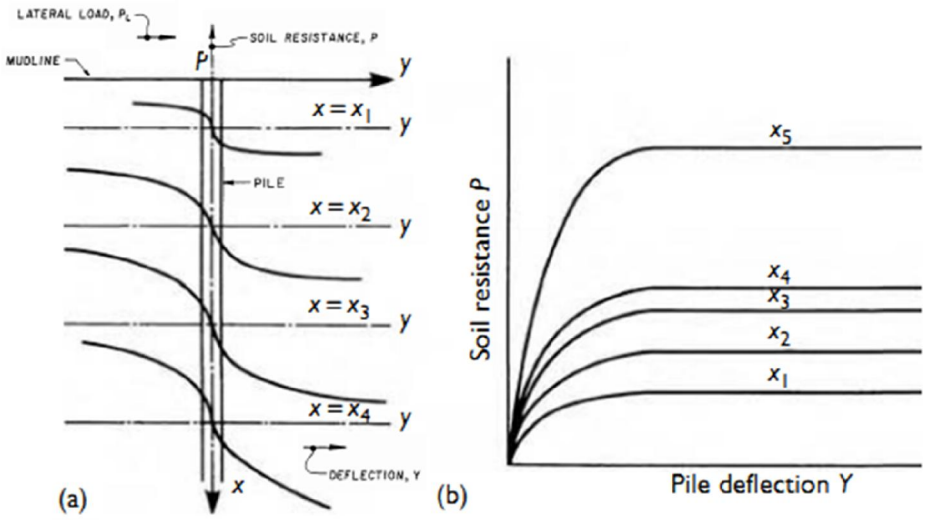

Figure 14: P-y Curve (a) Typical Set of p-y Curves for a given Soil Profile (b) curve plotted on common axes (Tomlinson & Woodward, 2008)

Radiation damping is the dissipation of energy in the soil-pile system because of the departing stress waves which transfer from pile-soil interface to infinity. Wang et al. (1998), Berger et al. (1977), and other researchers recommended an easier approach by supposing that the pile cross section only creates one dimensional P-waves

travelling in the direction of the shaking, and one dimensional S-waves travelling perpendicular to the pile as it shown in Figure 15a.

Novak et al. (1978) suggested a more accurate model by assuming a plain strain state for the soil which is linearly elastic, isotropic, and homogeneous. They have evaluated the pile experiencing uniform harmonic motions in an infinite medium. The problem become easier for 3D compared to 2D, due to the pile being regarded as rigid and infinitely long, without mass, like a stiff circular disc vibrating in an infinite elastic plane as shown in Figure 15b.

Gazetas and Dobry (1984a), (1984b) recommended a simplified model by supposing that compression-extension waves spread in the two fourth-parts planes along the direction of shaking, and that S-waves spread in the two fourth-parts perpendicular to the direction of shaking as presented in Figure 15c. From each of the previous methods, the coefficient of dashpot (C) can be concluded. A damper like this with (C) coefficient is settled in parallel with the non-linear spring element.

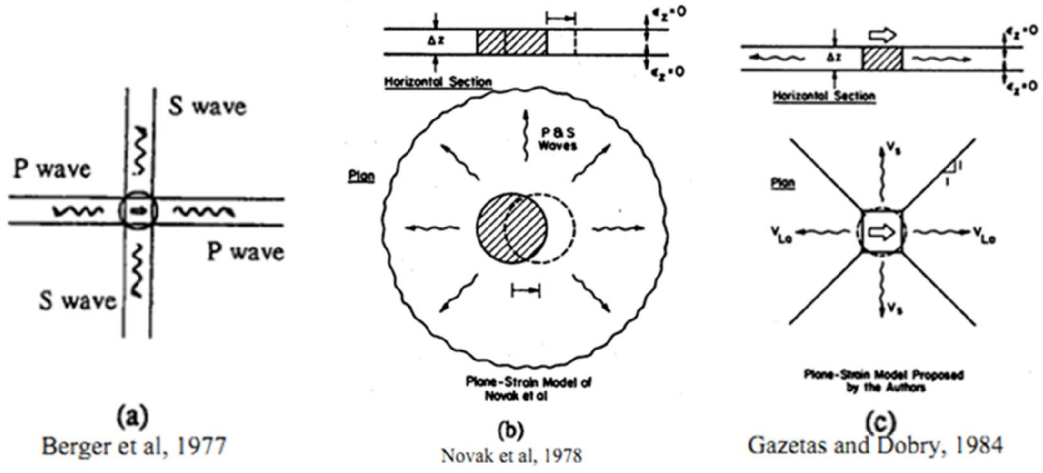

Figure 15: Model to Analyze Radiation Damping for a Horizontally Vibrating Pile (Wang et al., 1998)

Kagawa and Kraft (1980; 1981), and Badoni and Makris (1996) by using a BNWF (Beam on Nonlinear Winkler Foundation) presented a condensed modeling of damping and stiffness for a soil-pile system.

The BNWF method is a simple method which can use for nonlinear Soil Pile Structure Interaction (SPSI) and has verified applicable in professional engineering and investigate exercises. Various authors have suggested that the Winkler Model represents a Continuum Model on the assumption that the soil is an isolated horizontal plane in a plane strain condition of stresses.

As Nogami and Novak (1980) presented these solutions are extremely good estimations of the real 3D behavior for frequencies higher than basic natural frequencies of the soil deposit. To compute the linear response of single piles in bending, established up on the plane strain solutions, Nogami and Konagai (1988) recommended a time-domain method, with a series of springs and dashpots (presented in Figure 16, 17).

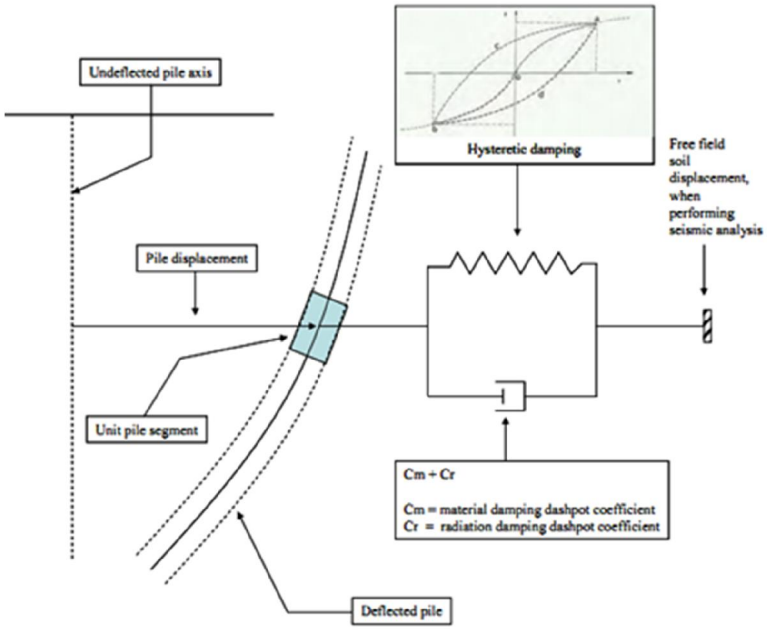

Figure 16: Beam on Nonlinear Winkler Foundation model with Different Damping Influences (Nogami & Konagai, 1988)

The moderated Winkler Model was verified for a large spectrum of frequencies, and occasionally mentioned as a Hybrid Dynamic Winkler Model (HDWM).

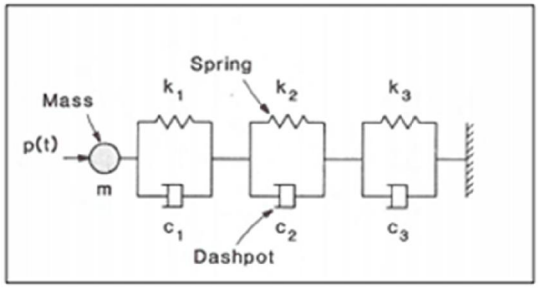

Figure 17: Hybrid Dynamic Winkler Model for Lateral Pile Response (Nogami & Konagai, 1988)

2.2.3 Finite Element Method

For static loading, Wolf (1985) defined an imaginary boundary at an adequate distance from the pile where it was expected that the response disappears from a feasible point of view, it is introducing as soil with finite domain. For boundary nodes, pin supports are allocated for restraining displacements, and the finite area is

meshed. This imaginary boundary can send back the waves produced by the vibrating pile due to dynamic loading, in to the defined soil medium. However, in reality it should be letting the waves propagate into infinity. More attention has to be paid in putting suitable damping capability at the boundaries of the soil finite element model. In the following paragraphs, a brief summary of some recent publications is presented which are used as references for this research. In the following paragraphs, a brief summary of some recent publications is presented which are used as references for this research:

A finite element model has been developed by considering the soil nonlinear behavior and introducing Drucker-Prager yielding criteria, wave scattering by putting the excitation at the bottom of the model, and discontinuity conditions at the soil-pile interface by introducing contact elements that enable to slippage (Bentley & El Naggar , 2000). They used this model for comparing the free-field soil reaction with the soil-pile system reaction, and dynamic soil-pile response. They applied earthquake excitations with low primary frequencies as an acceleration time history at the bedrock meshes, and they realized that the response of piles in elasto-plastic soil is almost similar to the free-field response to the low frequency seismic excitation.

Regarding the influence of material nonlinearity in the soil and separation at the soil pile interface on the dynamic response of a single pile and group piles, Maheshwari et al. (2004) proposed 3D finite element method to achieve the pile reaction under loading on the pile cap and seismic excitation. Figure 18 depicts the finite element meshing which Maheshwari et al. (2004) used.

Increasingly the Boundary Element Method (BEM) has been used in the laterally loaded piles evaluation. Ben Jamma and Shiojiri (2000) utilized a mix of finite element method and thin layer element for assessing the hybrid soil substructure system and the dynamic reaction of single pile driven in an infinite half space. Basile (2003) accounted on the advantages of the boundary element method for soil-pile interaction modeling and evaluation.

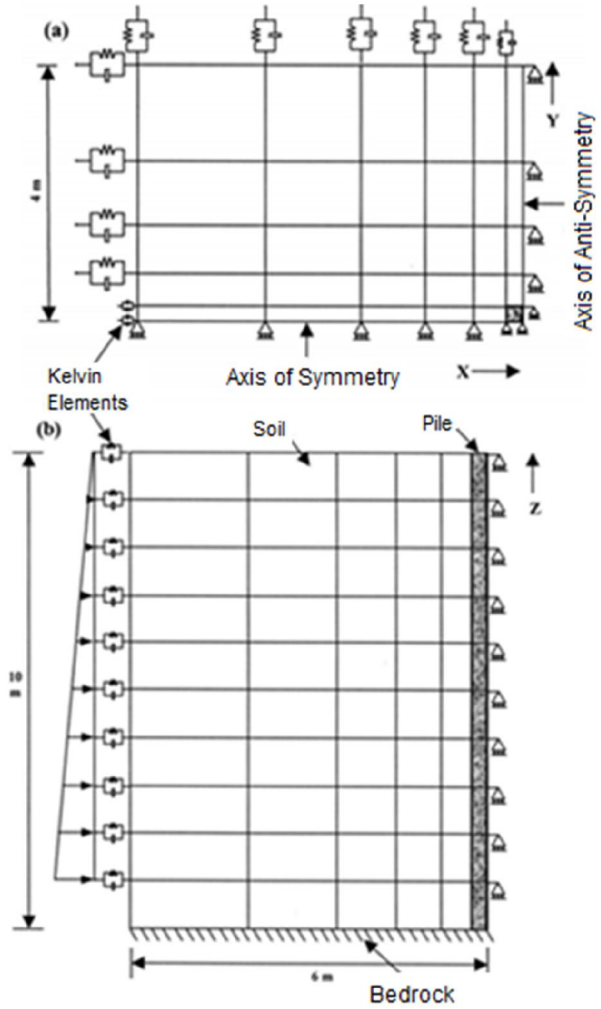

Figure 18: Finite Element Boundary Elements and Meshing for quarter model, (a) Top Plan of the Model, (b) Elevation (Maheshwari et al., 2004)

In recent times, researchers have begun to improve numerical analysis in which all the soil, piles, and soil pile structure interfaces are designed simultaneously together.

Angelides and Roesset (1980), Randolph (1981), Faruque and Desai (1982), Trochanis et al. (1991) and Wu and Finn (1997) utilized finite element method for pile dynamic analysis. Soil is treated as a continuum mass in FEM.

The earliest studies of dynamic response of piles and soil-pile interaction are in a consequence of Parmele et al. (1964), (Novak, 1974), Novak et al. (1978) to explain the dynamic elastic stress and displacements of fields by using a nonlinear discontinuous model and static hypothesis. Tajimi (1966) employed a linear viscoelastic bed layer to model the soil and he neglected the vertical part of the soil movement in his studying of the horizontal response. Novak (1974) supposed linearity and an elastic layer of soil made-up of independent thin horizontal layers reaching out to infinity.

Trochanis et al. (1988) utilized a three dimensional nonlinear analyze of piles to gain some insight of the lateral performance of piles, which led to the improvement of the simplified medol. In that study the ABAQUS (1987) was utilized. For soil, the Drucker-Prager inelastic model was used. The nonlinear soil behavior and the soil-pile gapping at their interface was evaluates for lateral and axial response of piles due to cyclic and monotonic loading. The piles were simulated as a concrete square cross-section. The results adapted with experimental field tests. It was carried out that interaction between neighboring piles was affected by nonlinear reaction, and neglecting these influences can obviously overestimate the amount of interaction between piles. It was found for lateral loadings, the plasticity of soil was a determinant factor influencing the horizontal response.

Trochanis et al. (1991) presented that the response of laterally loaded piles predicted utilized the ABAQUS modeling adapted with static load test data and 3D nonlinear finite element method. Boulanger et al. (1999) demonstrated that the results of seismic response of piles utilizing ABAQUS simulation with centrifuge experimental tests.

The objective is to find a precise solution for a complex problem by substituting it by a simple problem. The fundamental idea behind any finite element method is to divide the region, main part or structure being evaluated in to a large number of finite integrated elements. The key idea of finite element analysis is to (1) discretize complex region into finite elements and (2) use of interpolating polynomials to describe the field variable with in an element (Frank, 1985).

Zienkiewicz and Cheung (1967) were the first to present the implementation of the finite element methods to non-structural problems in the field of conduction heat transfer, but it was immediately accepted that the procedure was feasible to all problems that could be stated under variable form. These coincident improvements made the finite element analysis as one of the most powerful solution methods in recent times (Frank, 1985).

Today, the most versatile continuum-based method of analysis available is the finite element method. Various investigations have done on different forms of the finite element method (e.g., two-dimensional analysis, three-dimensional analysis, finite elements coupled with Fourier techniques) to evaluate laterally loaded piles [(Desai & Appel, 1976), (Randolph, 1981), (Kooijman & Vermeer, 1988), Trochanis et al. (1991), (Bhowmik & Long, 1991), (Bransby M. F., 1999)].

The other available continuum based methods are Baguelin et al. (1977), Pyke & Beikae (1984), Lee et al. (1987), Lee & Small (1991), Sun (1994), Guo & Lee (2001) and Einav (2005). These methods are feasible only to linear elastic soils, which do not demonstrate the real field conditions, these are seldom utilized by professionals due to the analysis include complex mathematics.

Brown and Shie (1991) presented a three dimensional analysis utilizing a simple elastic-plastic constant yield strength envelope (Von Mises Surface) to simulate a saturated clay soil and a modified Drucker-Prager model without associated flow rule for sands.

Chapter 3

METHODOLOGY

3.1 Introduction

The disastrous damage from recent earthquakes (e.g. Santiago 1985, Whittier Narrows 1987, Cairo 1992, Kobe 1995, Kozani-Grevena 1995, Yugoslavia 1998, Athens 1999, Kocaeli 1999, Bingol 2003, and Van 2009) has increased concern about the current codes and methods utilized for the design of structures and foundations. Many years ago, free field accelerations, velocities and displacements have been utilized as input grand motions data for the seismic design of foundations and structures without mentioning the kinematic interaction of the foundation that have carried out from the introduction of piles and the soil geology.

According to the pile group design and soil profile, free-field response may underestimate or overestimate real in-situ conditions which as a result, will fundamentally change design criteria. Kinematic and Inertial are the two basic loading conditions of earthquake induced loadings. Fan et al. (1991) carried out a considerable parametric study by utilizing an equivalent linear approach to improve dimensionless diagrams for pile head deflections versus the free field response for different soil profiles under perpendicular propagating harmonic waves.

By cooperating frequency-dependent springs and dashpots to analyze the single pile and group piles response, Maluis and Gazetas (1992) indicated free-field acceleration

to a one dimensional Beam-on-Dynamic-Winkler-Foundation model. Both researches studies that the influences of interaction on kinematic loading are insignificant. However the interaction effects are significant for pile head loading. These studies were limited to linear analysis and one-dimensional harmonic loading.

In this thesis a 3D nonlinear dynamic and static analysis were performed to evaluate the effect of slenderness ratio on lateral deflection of pile under lateral loading and the input motion (wavelet) on the foundation. The finite element program ABAQUS was utilized in this analysis.

ABAQUS is a powerful finite element computational simulation tool widely used both in the academic environment and industry, and its absorbing feature to researchers and advanced users is the available option to implement user-defined elements, materials, load and boundary types, etc. through user-defined subroutines. These subroutines may be written in FORTRAN, C or C++ languages. These subroutines may be linked to ABAQUS through various ways depending on one's preference and the operating system.

The ABAQUS finite element program can solve dynamic response of structural systems one of the frequency domain or time domain which the time domain was chosen for current study.

Static analysis process took approximately 45 minutes and more, however the dynamic analysis needed much more time. For Ricker wavelet with 0.002 second time intervals, the nonlinear analysis took approximately 1 day on a Pentium 4

personal computer with Dual-Core 2.6 GHZ CPU and 3GB RAM, which were utilized at Eastern Mediterranean University.

3.2 Assumptions and Limitations

The present system consists of a pile foundation supporting a structure. As one-dimensional horizontal acceleration, the dynamic loading was applied to the underlying bedrock (X-direction in the model) and the vertical and horizontal responses were evaluated. Due to boundaries of safety against vertical static forces, commonly provided sufficient resistance to dynamic forces caused by vertical accelerations, vertical accelerations were neglected. Wu and Finn (1996), concluded that deformations in the vertical direction are negligible compared to deformations in the horizontal direction of shaking by utilizing three dimensional elastic model.

The liquefaction potential is not mentioned in the current analysis, but the dilatation effect of sands around the piles is considered. Additionally drained conditions were adopted; hence the excess pore pressures were not taken into account.

3.3 Three Dimensional Finite Element Model

3.3.1 Mode1 Simulation

Soil-pile systems were illustrated with full 3D geometric models. One half of actual model was simulated; due to the advantage of symmetry in reducing the computing time. Figure 19 shows an isometric view of the half of pile-soil system which was utilized in the system. In both of pile and soil model eight-nodes elements were used.

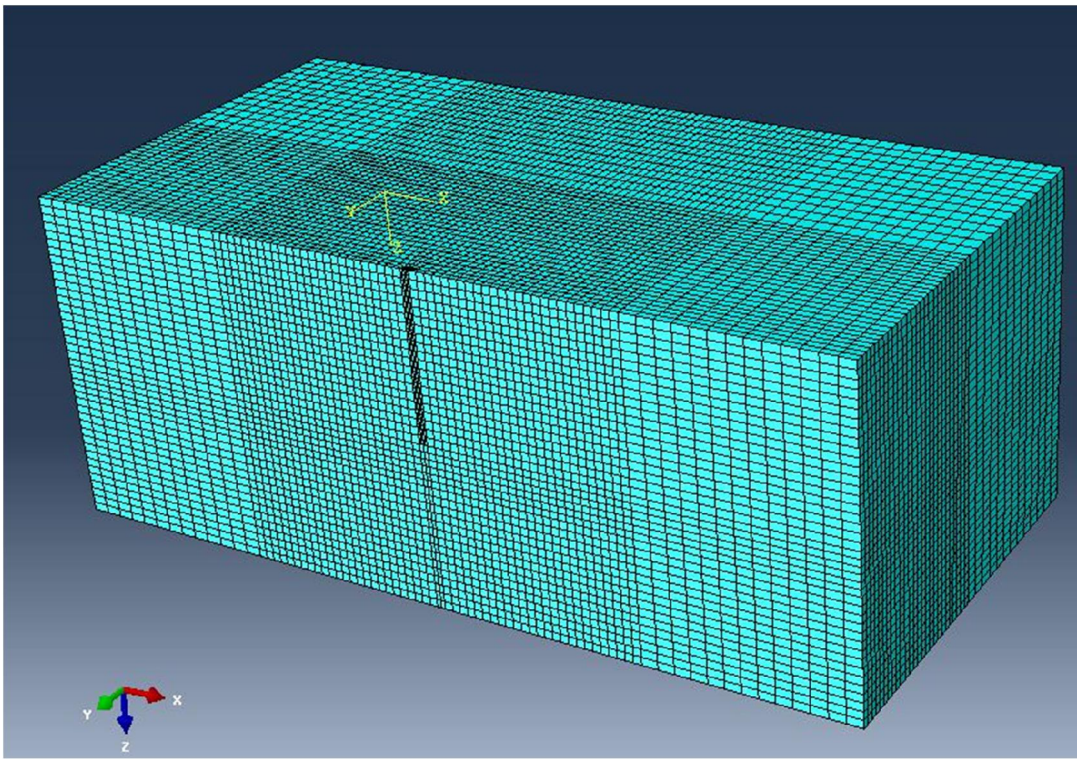

Figure 19: Overall view of the half of pile-soil system with mesh

To avoid the "box effect" (meaning that the waves being reflected back into the model from the boundaries) through the dynamic loading, transmitting boundaries were utilized to enable the wave to propagate. Infinite elements were defined for simulating the transmitting boundary.

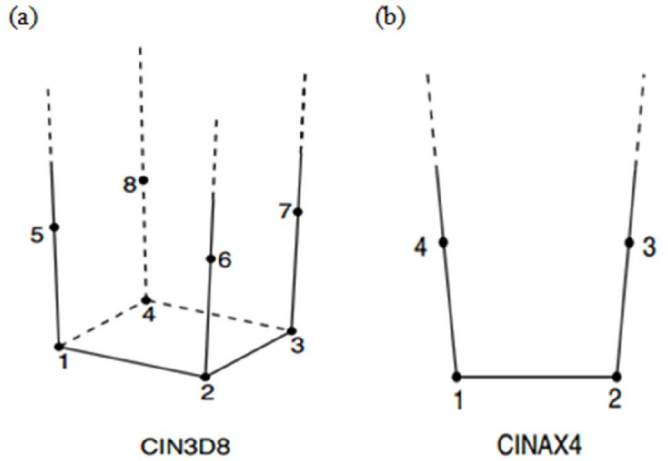

Figure 20: Schematic of Infinite Elements (a) Three-Dimension Solid Continuum Element, (b) Axisymmetric Solid Continuum Element (ABAQUS, 2010)

3.3.2 Soil Properties

The soil was simulated as elastic and elasto-plastic. For analyzing the influence of soil plasticity on the response, a homogeneous elasto-plastic material using Drucker-Prager failure criteria have been utilized (Chen & Mizumo, 1990). For cases including plasticity, the dilatation angle was assumed to be unequal to the friction angle (non-associated flow rule). Excess pore water pressures were not considered (drained condition).

The dilatation angle for sand depends both on the density and the angle of internal friction and a small negative value of dilatation angle is realistic for loose sand (Nag Rao, 2006). A basic equation for dilatation angle and the friction is shown in Equation 3.1.

$$\Psi \approx \varphi - 30^0 \tag{3.1}$$

3.3.2-1 Drucker-Prager Model

Utilizing Cam Clay modeling for sand has not achieved any success. The cause was that the experimental plastic potential was completely antithetic from the experimental yield locus, as recommended first by Poorooshasb et al. (1967) who were the first to assess the problem of achieving the soil specimen deformation under a present stress increase as an incremental elasto-plastic problem.

Fundamental modeling of soil behavior under general loading and different site conditions is the important factor to achieve accurate numerical outcomes. A linear elastic basic relationship has been widely utilized to depict soils in early numerical researches; but most soil behavior is highly nonlinear. In this chapter, a brief

explanation about plastic theory is given and then the extended version of Drucker-Prager plasticity model is demonstrated in detail.

ABAQUS provides a large number of plasticity models to incorporate soil nonlinearity in the analysis. These include the Extended and Modified Drucker-Prager models, the Mohr-Coulomb plasticity model and the Critical state (clay) plasticity model. These are sophisticated plasticity models that require calibration based on experimental data. There is a short description of the Drucker-Prager soil model used in this thesis.

The Drucker-Prager plasticity model was recommended by Drucker-Prager (1952) for frictional soils. The plasticity theory and failure criterion model are illustrated in the following subsections.

The extended Drucker-Prager models are used to model frictional materials, which are typically granular-like soils and rock, and exhibit pressure-dependent yield (the material becomes stronger as the pressure increases).

(a) Plasticity approach

Soil deformation includes elastic and plastic strains relating to loading and unloading ways. Plastic behavior is taken into account as soil irrecoverable deformation while elastic is considered the behavior when deformation is recoverable. Incremental approach of plasticity has been utilized successfully in depicting of a wide range of materials such as soils.

(b) Soil failure surfaces

Many experiments carried out on different sands at various confining pressures showed the general shape of the failure surface as presented in Figure 21. In

numerical soil models the shape of the failure surface should be the same as shown in Figure 21.

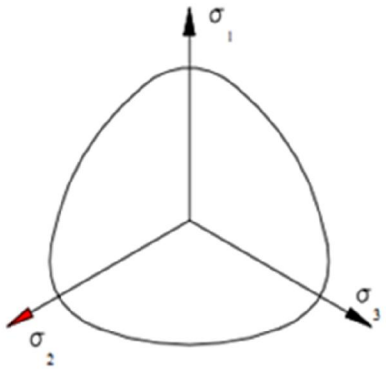

Figure 21: Failure surface for sand in the deviator plane (ABAQUS, 2010)

In Figure 22 four common soil models are demonstrated together with the general shape of the failure model for sand.

According to overestimating of the tensile strength and the sharp corner which present singularities, the Extended Tresca does not set a satisfactory shape of failure compared to the general failure surface. The Mohr-Coulomb accuracy has been well documented for many soils, and the simplicity of this model is one of the advantages of it.

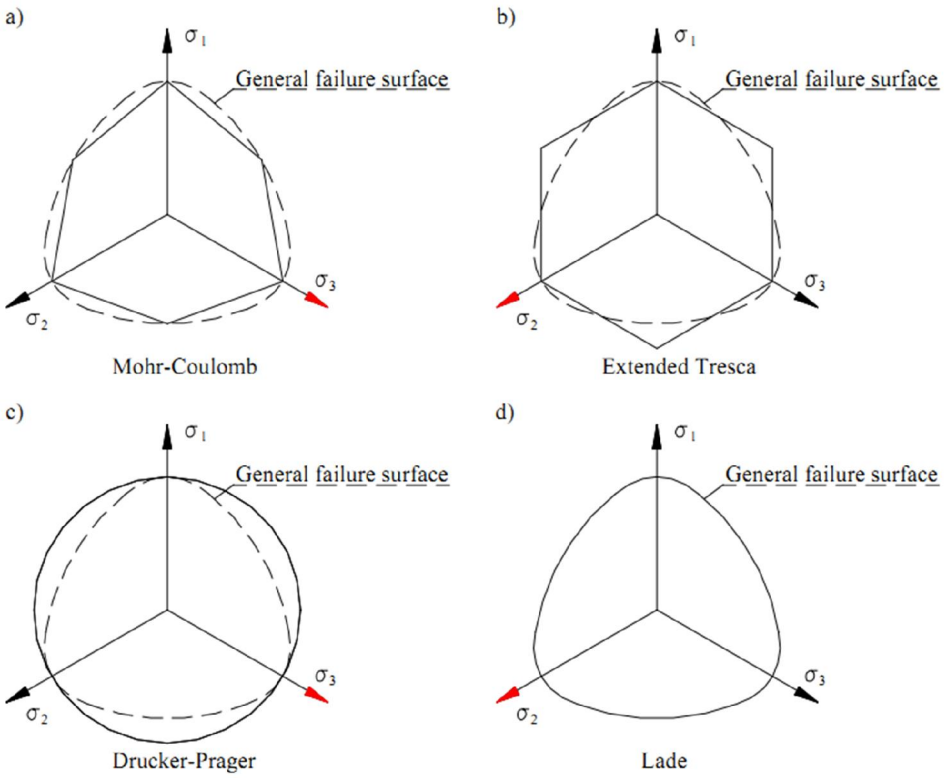

Figure 22: Deviator plane failure surfaces for two parameter models (ABAQUS, 2010)

Neglecting the effect of the intermediate principal stress (σ_2), and non-mathematical adapted in the three dimensional application because of the presence of corners, which simulate singularities, are the Mohr-Coulomb model primarily disadvantages (Chen & Baladi, 1985).

Chen and Liu (1990) demonstrated the smooth Drucker-Prager model by improving the Von-Mises failure criterion. This model is appropriate to use due to the failure surface being smooth, and with convenient material constants it can adapt with the Mohr- Coulomb criterion obtained from triaxial tests.

As it can be seen in Figure 22c the Drucker-Prager is circular in the deviator plane and the general failure surface has a “soft” triangular form. Regarding to the soil

strength, it should be expected that the Drucker-Prager model overestimates the tensile strength with some uncertainty. Instead of this, the Lade failure model could be used, due to the high accuracy in predicting the general failure surface.

According to the accessibility of the Drucker-Prager model in the present ABAQUS version, this model is used although there is a lack of accuracy at failure. The material input data can be obtained from triaxial test.

(c) Drucker-Prager failure model

Equation 3.2 shows the failure function of Drucker-Prager materials involving the hydrostatic effect on the shearing resistance:

$$f = \sqrt{J2} - \alpha . I_1 - K = 0 \tag{3.2}$$

where "I_1" is the first principle stress constant, "J_2" is the second deviator stress constant, and "α" and "k" are material invariants which relates to the friction angle and cohesion, consecutively.

In Equation 3.2, when" f" is equal to zero the material will follow the plasticity flow rule, meaning it goes through both elastic and plastic strain, and when it is less than zero the material will only go through elastic strain.

- f < 0 Ideal elastic behavior.
- f = 0 Elasto-plastic behavior.

Chen and Baladi (1985) illustrated that the plastic deformation of Drucker-Prager material is followed by a volume expansion which represents a uniform dilation. In Figure 22a it is evident that when the elasto-plastic behavior is mentioned, it is controlled by plastic flow rule, which again controls the hardening of the material.

As it is demonstrated in Figure 22a the Drucker-Prager model utilizes isotropic hardening behavior.

The Drucker-Prager is linear in the constant $\sqrt{J2}$, $(I_1/3)$ space, as presented in Figure 23. Since frictional materials are cohesionless by nature, this is not a good description of the hardening behavior. This is a result of Drucker-Prager needing cohesion to define the yield stress where elasto-plastic behavior sets in.

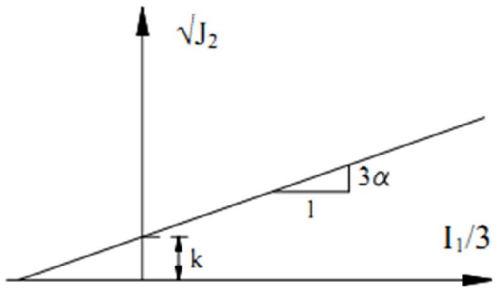

Figure 23: Drucker-Prager failure surface (ABAQUS, 2010)

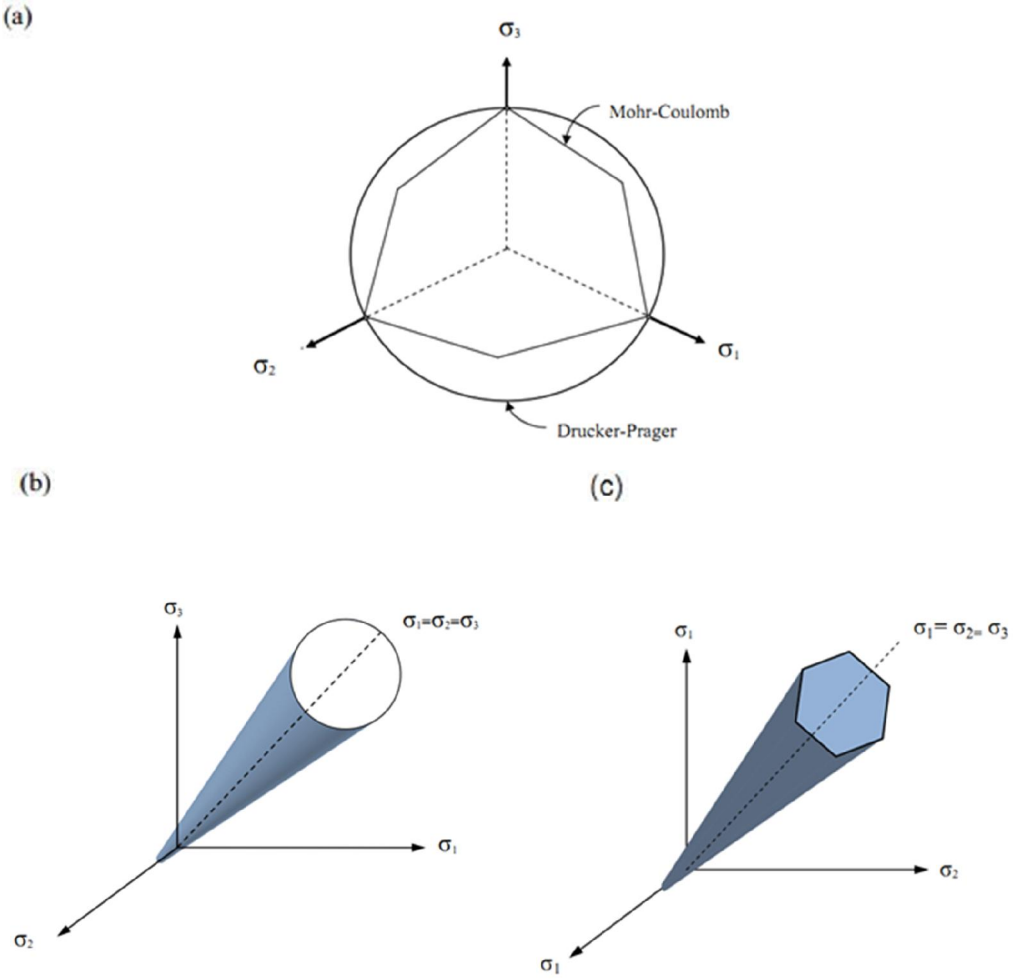

Figure 24: Yield Surfaces on a Deviator Plane (a) Drucker-Prager and Mohr-coulomb yield surfaces on deviator plane, (b) the Drucker-Prager failure surface on a deviator plane, (c) Mohr-Coulomb yield criterion on a deviator plane (Serdaroglu, 2010)

Table 2: The advantages and limitations of Mohr-Coulomb and Drucker-Prager models

Fundamental Model	Advantage	Limitations
Mohr-Coulomb		
	Simple	Yield surface has corners
	Valid for many soil types	Neglect the effects of intermediate principal stress
	Model parameters can be obtained easily from soil experiments	
Drucker-Prager	Simple to use	Excessive plastic dilatancy at yielding
	Can be matched with Mohr-Coulomb model	Cannot produce the hysteretic behavior within the failure surface
	Analysis techniques can be implemented	Cannot predict the pre pressure build-up during an undrained cyclic shear loading
	Satisfy the associated flow rule	

In nature the elasto-plastic behavior exists throughout the loading period, which implies that the hardening behavior should be defined as illustrated in Figure 25b. By defining hardening as depicted in the figure, the influence of the cohesion on the failure surface is excluded, and this is modeled by the "Mobilized Friction Model" (Jostad et al. (1997).

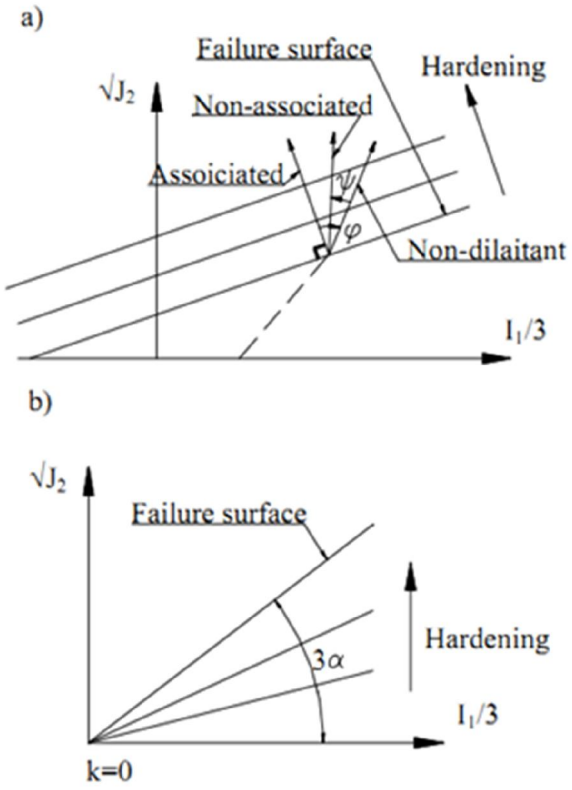

Figure 25: Hardening behavior, (a) Drucker-Prager, (b) common (Jostad et al. (1997))

(d) Drucker-Prager soil model in ABAQUS

This part includes an explanation of Drucker-Prager model in ABAQUS. The terminology and sign definition used in this part are exactly the same as the the ones utilized in the ABAQUS manuals. There are three various models of Drucker-Prager in ABAQUS, which are, "Linear model", "Hyperbolic model", and "Exponential model". In this thesis the Linear Drucker-Prager model is chosen. The linear

Drucker-Prager criterion is defined in Equation 3.3 in ABAQUS, which is also depicted in Figure 26 (ABAQUS, 2008).

$$f = t - p\tan\beta - d = 0 \tag{3.3}$$

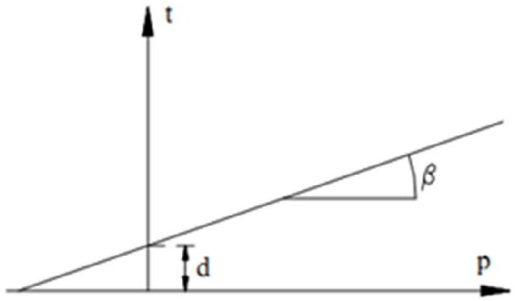

Figure 26: Linear Drucker-Prager (ABAQUS, 2008)

where "p" is the equivalent pressure stress (mean stress), "β" and "d" are the friction and cohesion factors, respectively while "t" is the generalized shear stress, determined as shown in Equation 3.4.

$$t = \frac{1}{2}q\left[1 + \frac{1}{K} - \left(1 - \frac{1}{K}\right)\left(\frac{r}{q}\right)^3\right] \tag{3.4}$$

where "q" is the Von-Mises equivalent stress, "r" is the third constant of the deviator stress and "K" is a factor that clarifies the ratio between the yield stress in triaxial compression and tension. The cohesion factor, "d", is determined from:

$d = \left[1 - \frac{1}{3}.\tan(\beta)\right].\sigma_c$ if hardening is defined by the uniaxial compression yield stress, σ_c

$d = \left[1 - \frac{1}{3} . \tan(\beta)\right] . \sigma_t$ if hardening is defined by uniaxial tension yield stress, σ_t

The parameters β and d can be adapted with the Mohr-Coulomb parameters for two different cases (flow associated and non-associated rule) which are summarized in Table 3.

Table 3: The relationship between Drucker-Prager material constants and the Mohr-Coulomb parameters (Serdaroglu, 2010)

Flow Rule	Drucker-Prager Material Constants	
Associated Flow Rule, $\psi = \Phi$	$\tan\beta = \frac{\sqrt{3}.\sin\varphi}{\sqrt{1+\frac{1}{3}sin^2\varphi}}$	$d = \frac{\sqrt{3}.\cos\varphi}{\sqrt{1+\frac{1}{3}sin^2\varphi}}$
Non-Associated Flow Rule, $\psi \neq \Phi$	$\tan\beta = \sqrt{3}.\sin\varphi$	$d = \sqrt{3}.\cos\varphi$

The "K" factor defines the ratio between the yield stress in triaxial compression and tension, and herewith the yield surface is shaped by "K" in the intermediate stresses. When the triaxial tension is equal to the triaxial compression, (K=1) and (t=q), and the yield surface is equal to the Von-Mises circle in the deviator principal plane. To ensure the surface is convex, it is required that $0.778 \leq K \leq 1$. Figure 27 is the proof of this part.

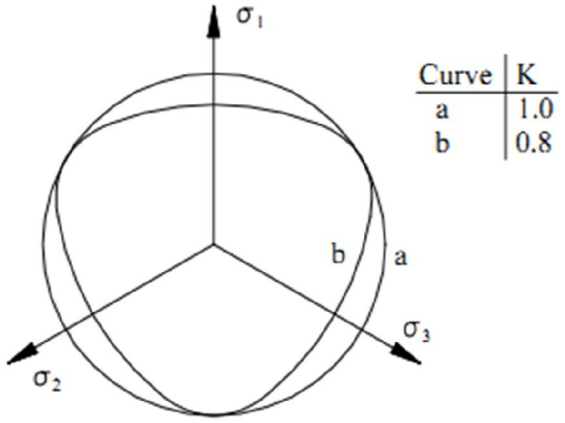

Figure 27: Drucker-Prager Yield surface from ABAQUS (2008)

As pointed out in Figure 28, for granular materials, such as sand, the linear model is normally used with the non- associated flow, $\psi \neq \Phi$.

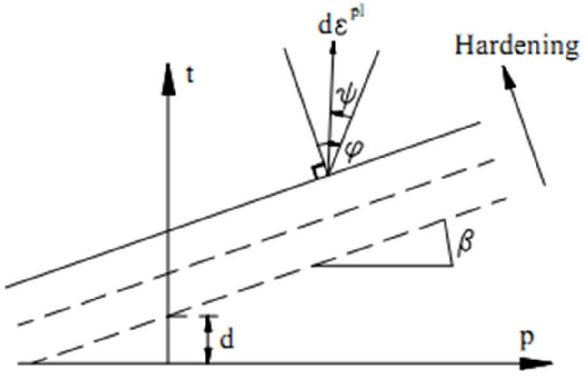

Figure 28:Yield Surface and Plastic Flow direction in the p-t plane from (ABAQUS,2008)

The material damping ratio of the soil, ζ, was assumed to be 5% based on average cyclic shear strain laboratory tests (Kramer, 1996). The general equation of the system is presented by Equation 3.5.

$$[M]\{\ddot{u}\}+[C]\{\dot{u}\}+[K]\{u\}=\{F(t)\} \tag{3.5}$$

where $\{\ddot{u}\}$ is the acceleration vector, $\{\dot{u}\}$ is the velocity vector and $\{u\}$ is the displacement vector {F(t)} is total force, and [M], [C] and [K] are the global mass, damping matrice and stiffness matrice, respectively. The damping matrix, [C] = β [K], where β is damping coefficient $\beta = \frac{2\zeta}{\omega_0}$, and the predominant frequency of the loading (rad/sec) is substituted for natural frequency (ω_0).

3.3.3. Pile Properties

Concrete cylindrical section pile with linear elastic properties was used in this study. The pile was simulated utilizing 8-noded brick elements.

3.3.4 Soil-Pile Interface

The soil-pile interface modeling is very important due to its influence on the pile response under lateral loading Trochanis et al. (1988). In the soil-pile interaction, the surrounding soil and the pile elements are assumed deformable. The surface of pile elements and soil elements have contact, which the surface of pile elements are selected as “Master surface” and the surfaces of soil elements are defined as “Slave surface” . In ABAQUS these surfaces are called the contact pair and they are depicted in Figure 29. Figure 30 presents the simulated model’s master and slave surface in this study.

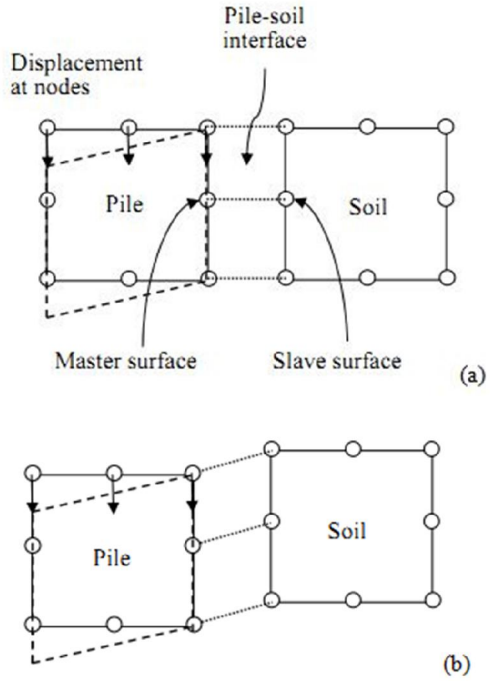

Figure 29: Schematic FEM Soil-Pile interface Elements, (a) No sliding, (b) Sliding

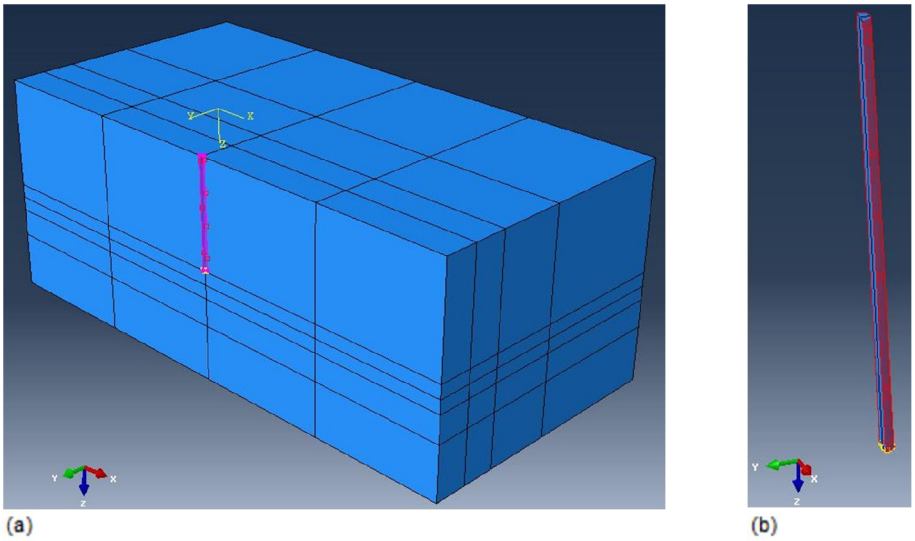

Figure 30: Interface between Soil and Pile, (a) Slave surface, (b) Master surface

Following the suggestions made by API (1991) and Gireesha (2011), the coefficient of friction between concrete and sand relating shear stress to the normal stress was

assumed to be 0.7 throughout the analysis. The "penalty function method" was utilized to represent the contact with normal contact stiffness (K_n).

3.4 Boundary Conditions

The boundary conditions differ according to the type of loading. In static analyzing the bottom of the model which demonstrates the top of the bedrock layer was fixed in all directions. However the top face of the model was free to move in all directions in both static and dynamic analyzing. The symmetry surfaces were free to move on the surface of the symmetry plane, but fixed against the normal displacement to the plane. In order to illustrate a horizontally infinite soil medium during static and dynamic analysis, the elements along the sides of the model were simulated as Kelvin elements (spring and dashpot), and they were free to move in vertical direction (Figure 31).

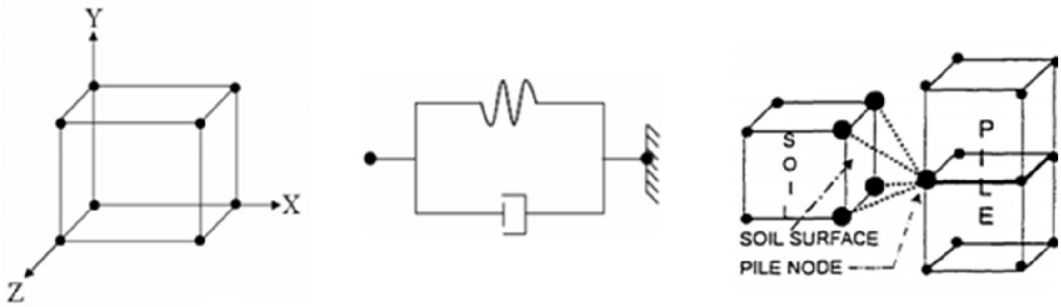

(a) Eight-nodded Element (b) Two-nodded Kelvin Element (c) Five-nodded Contact

Figure 31: Kelvin Elements (ABAQUS, 2010)

3.5 Loading Conditions

3.5.1 Static Loading

It should be noted that all static loads are applied as concentrated loads on the pile head. In this study, because of the symmetric geometry of pile, only half of the load was applied to the pile in the FEM analysis.

In this part the lateral deflection of pile head was evaluated under lateral loading which was applied on pile head. According to solid mechanics formulations the amount of lateral deflection can be obtained from Beam Flexure Theory. The pile which is placed in soil continued up to the bed rock or stiff layer, hence it can be considered as a cantilever beam (Bentley K. J., 1999), Equation 3.7 and Figure 32 are presented this theory.

$$\delta = \frac{PL^3}{3EI} \tag{3.7}$$

where:

δ: Horizontal deflection of pile head

P: Static lateral load

E: Modulus of elasticity

I: Moment of inertia

L: Pile length

This formula is used for verification of the ABAQUS results in soil elasticity.

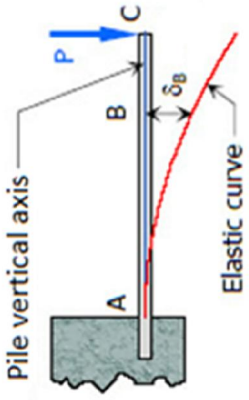

Figure 32: Pile schematic as a cantilever beam, a point as a bedrock

3.5.2 Dynamic Loading

For dynamic part to simulate the seismic wave, the Ricker SV wavelet described by Equation 3.8, representing the source function and frequency content, is utilized (Ricker, 1960). Elastic soil treatment is used in this simulation.

$$f\left(t\right)=[1-2\left(\pi.f_{p}.\left(t-t_{0}\right)\right)^{2}]\exp[-(\pi.f_{p}.(t-t_{0}))^{2}] \tag{3.8}$$

where:

f (t): amplitude,

f_p : predominant frequency in Hz,

t_0 : time parameter of time history in second,

A wavelet is utilized to represent a short time series and simulating a source function. The wavelets can be described as having amplitude in the frequency domain, and a time series in the time domain analysis. There are an infinite number of time domain wavelets for each amplitude spectrum which can be constructed by different type of phase spectrum. There are 4 typical wavelets named as Ricker, Ormsby, Klauder, and Butterworth. The Ricker wavelet is one of the particular type of wavelets which is usually utilized for simulating the excitation function which propagates vertically and it is distinguished by its dominant frequency. This wavelet is employed because it is simple to understand and often seems to represent a typical earth response.

The predominant frequency and time interval are considered 2 Hz, 0.002 sec, respectively in this study, which represent a typical destructive earthquake. Figure 33 presents the Ricker wavelet used in this study. Figure 34 is a schematic diagram of the seismic wave propagation from bedrock.

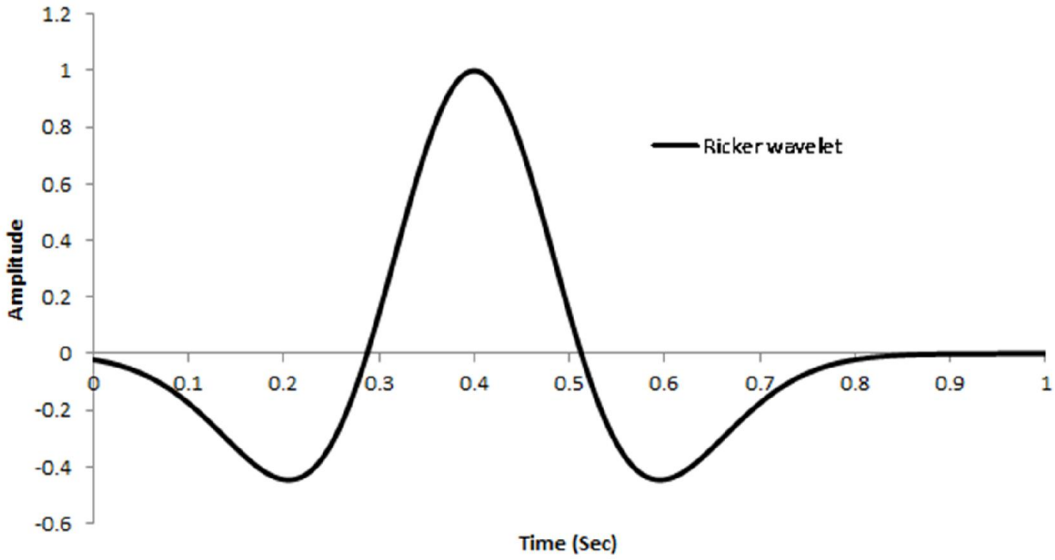

Figure 33: Ricker wavelet used in present elastic medium dynamic analysis

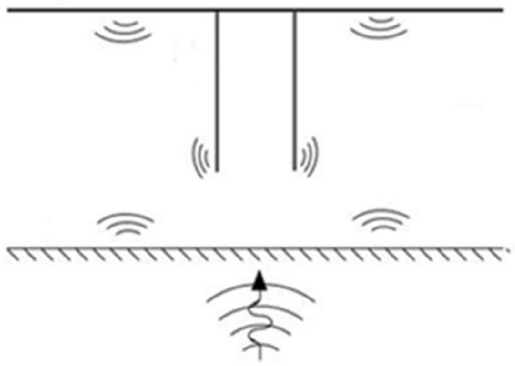

Figure 34: Schematic of the seismic excitation wave that comes through existing rigid bedrock

3.6. Verification of Finite Element Model

To guarantee that pile, soil, and boundary conditions were distinctly calculated to minimize error accruement, the verification process was adopted in incremental steps. Figure 35 is depicts the pile mesh model. The mesh density near the pile was larger than the other regions because of the severe stress gradients, as shown in Figures 36 and 37.

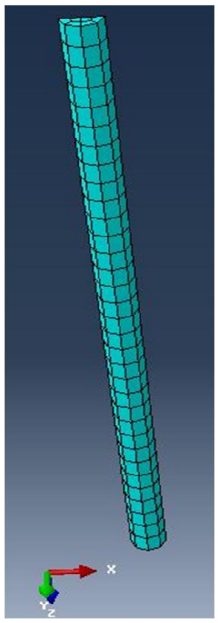

Figure 35: Simulated pile with mesh

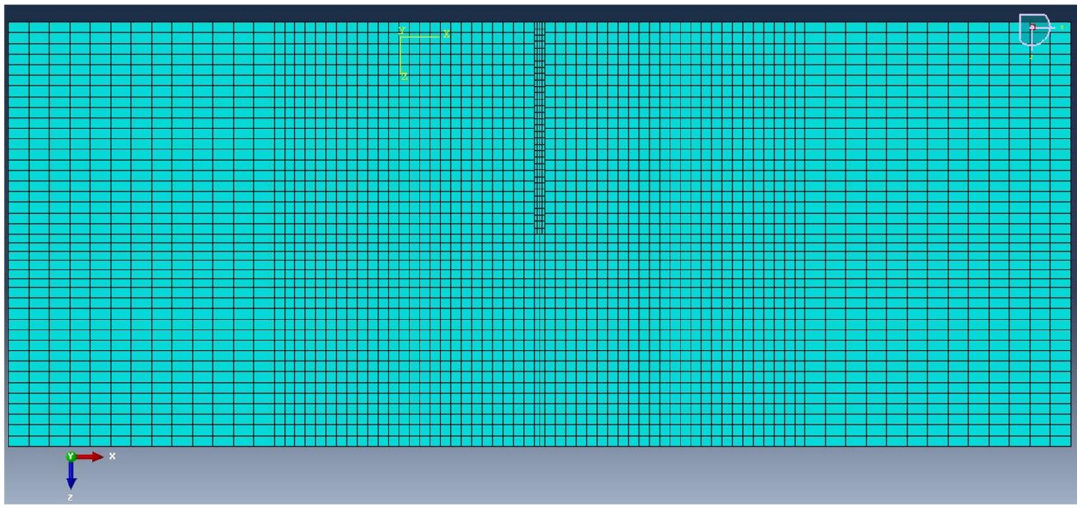

Figure 36: Plane x-z of soil-pile model shows the mesh density near the pile

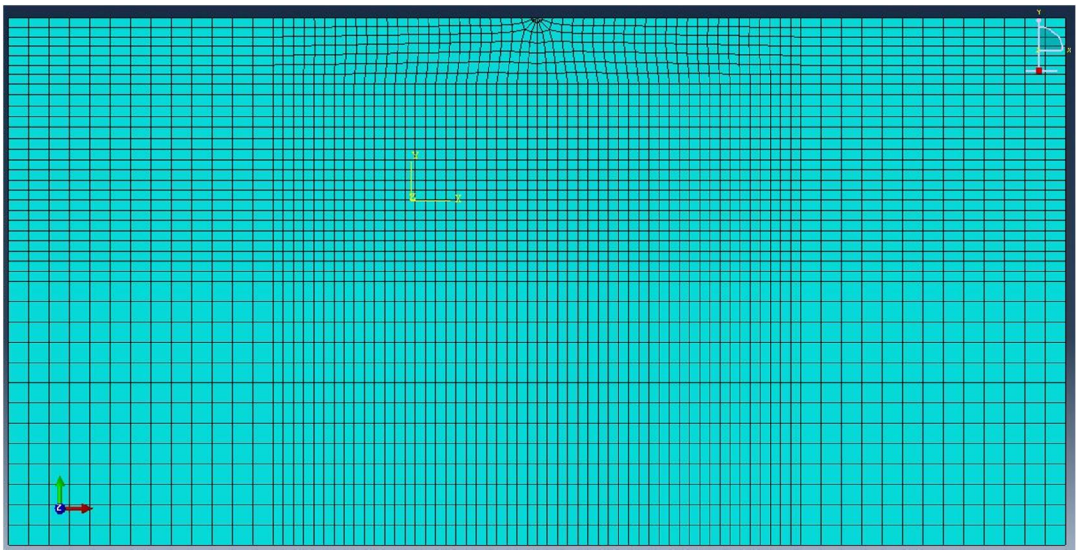

Figure 37: Top side of soil-pile model shows the mesh density around the pile

Chapter 4

NUMERICAL MODELLING

4.1 Introduction

In this chapter, the extended models for three dimensional conditions are employed in finite element analysis utilizing ABAQUS / CAE V 6.11. Information about methods used for modeling was discussed in Chapter 3. This chapter includes the estimation of parameters and simulation.

The critical location in lateral deflection is the pile head, mainly pile lateral deflection is considered here. Due to greater deflection of the upper part of piles and their capacity to carry higher lateral loads than lower parts; under lateral loading, the most critical part of the pile is the upper part (Poulos & Davis, 1980).

4.2 Model Description

4.2.1 Pile and Soil Properties

The soil used in this numerical study is standard medium sand, which is simulated as an elastic medium and elasto-plastic medium by Drucker-Prager material model with non-associated flow rule, which is explained by angles of friction and dilatation. The following parameters are used for sand: friction angle $\Phi = 32°$, Young's Modulus E = 2e+4 (kPa), Poisson's ratio ν = 0.45, unit weight γ = 1.5 (kN / m^3) and a dilation angle of $\psi = 2°$.

Table 4 shows all the model details which were studied in this thesis. A single concrete pile with circular cross section in two slenderness ratios of 10 and 20 and for each slenderness ratio different lengths and diameters were used. All properties and details of the employed materials are summarized in Tables 4-6. Four different static lateral loads were applied on the pile head for each case.

Table 4: All model details

Models No.	Pile Type	Soil Type	Analyzing Type	Load	L (m)	D (m)
1	Circular / Concrete	Sand /Elastic	Static	50, 100, 150, 200 kN	3	0.3
2	Circular / Concrete	Sand /Elastoplastic	Static	50, 100, 150, 200 kN	3	0.3
3	Circular / Concrete	Sand /Elastic	Static	50, 100, 150, 200 kN	5	0.5
4	Circular / Concrete	Sand /Elastic	Static	50, 100, 150, 200 kN	7	0.75
5	Circular / Concrete	Sand /Elastic	Static	50, 100, 150, 200 kN	9	0.9
6	Circular / Concrete	Sand /Elastoplastic	Static	50, 100, 150, 200 kN	9	0.9
7	Circular / Concrete	Sand /Elastic	Static	50, 100, 150, 200 kN	6	0.3
8	Circular / Concrete	Sand /Elastoplastic	Static	50, 100, 150, 200 kN	6	0.3
9	Circular / Concrete	Sand /Elastic	Static	50, 100, 150, 200 kN	10	0.5
10	Circular / Concrete	Sand /Elastic	Static	50, 100, 150, 200 kN	15	0.75
11	Circular / Concrete	Sand /Elastic	Static	50, 100, 150, 200 kN	18	0.9
12	Circular / Concrete	Sand /Elastoplastic	Static	50, 100, 150, 200 kN	18	0.9
13	Circular / Concrete	Sand /Elastic	Dynamic	Ricker wavelet	5	0.5
14	Circular / Concrete	Sand /Elastic	Dynamic	Ricker wavelet	10	0.5

Table 5: Pile and Geotechnical Properties

Parameters	Symbol	Soil	Pile	Unit
Unit Weight	γ	1.5	2.3	kN / m^3
Young's Modulus	E	2e+4	2e+7	kPa
Poisson's Ratio	ν	0.45	0.3	-
Friction Angle	Φ	32	-	Degree
Dilatation Angle	□	2	-	Degree

Table 6: Details of Model

Pile Details		Soil Details	
Size	(L / D)=10, (L / D)=20	Size of Block	50 x 50 m^2
Length & Diameter	Varied	Height	20 m
Type of Pile	Concrete	Type of Soil	Sand

4.3 Static Analysis Results

Figure 38 presents the comparison between ABAQUS results in elastic behavior of soil and Beam Flexure Theory, given in Equation 3.7.

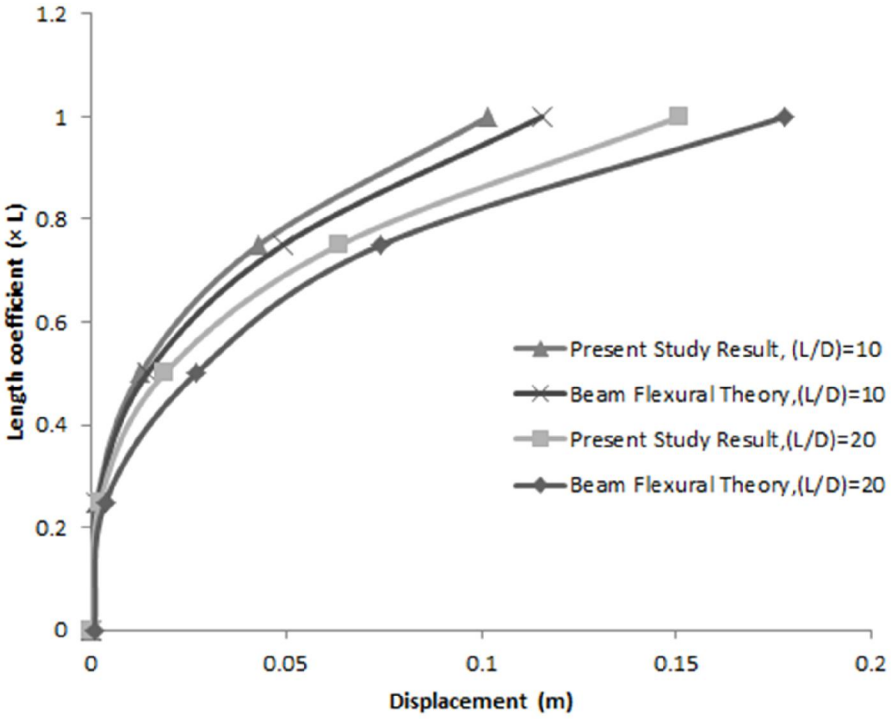

Figure 38: Comparison between Beam Flexure Theory and ABAQUS result

Comparing the numerical results in elastic and elasto-plastic behavior of soil, it is significant that the result of elastic behavior of soil is close to beam flexural theory. However the lateral deflections are higher in the elasto-plastic medium than the elastic medium. The beam flexural theory is defined by considering the elastic condition parameter (E) and geometric properties of pile (L, I). There are some differences between beam flexural theory and numerical results as shown in Figure 38. It is because of the lateral soil pressure around the pile which shows that there is no complete fixity for end of pile.

Figures 39 to 42 illustrate lateral deflection of pile with slenderness ratio of 10, at different depths along the pile shaft from the bottom (0.25L, 0.5L, 0.75L, L), under different lateral loads (50, 100, 150, 200 kN) in soil with elastic behavior.

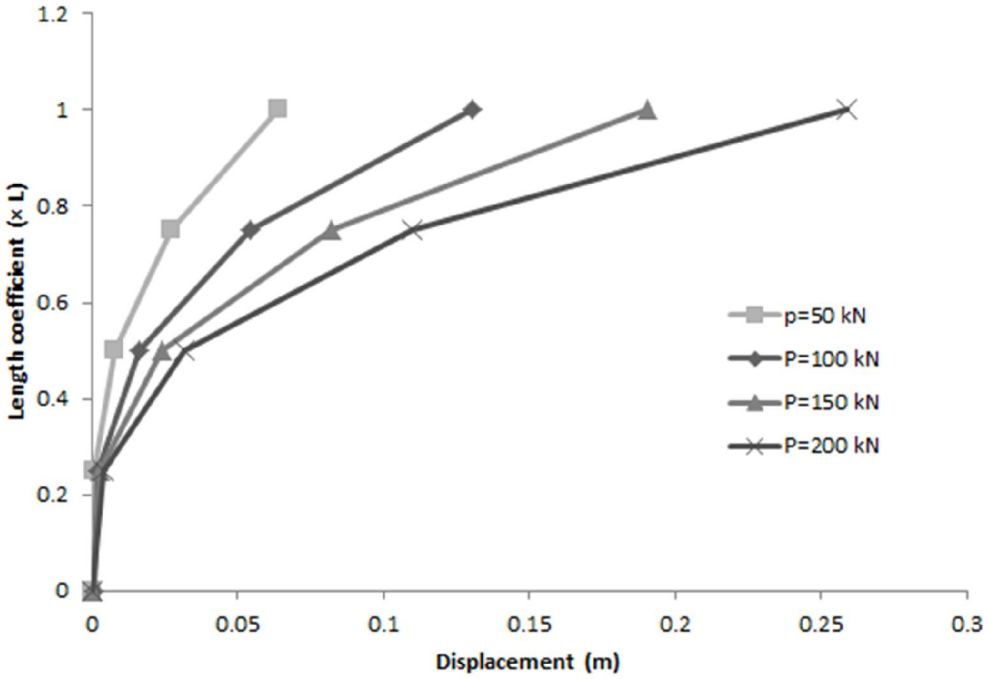

Figure 39: Lateral deflection of pile head in different depth of pile, L=3, D=0.3

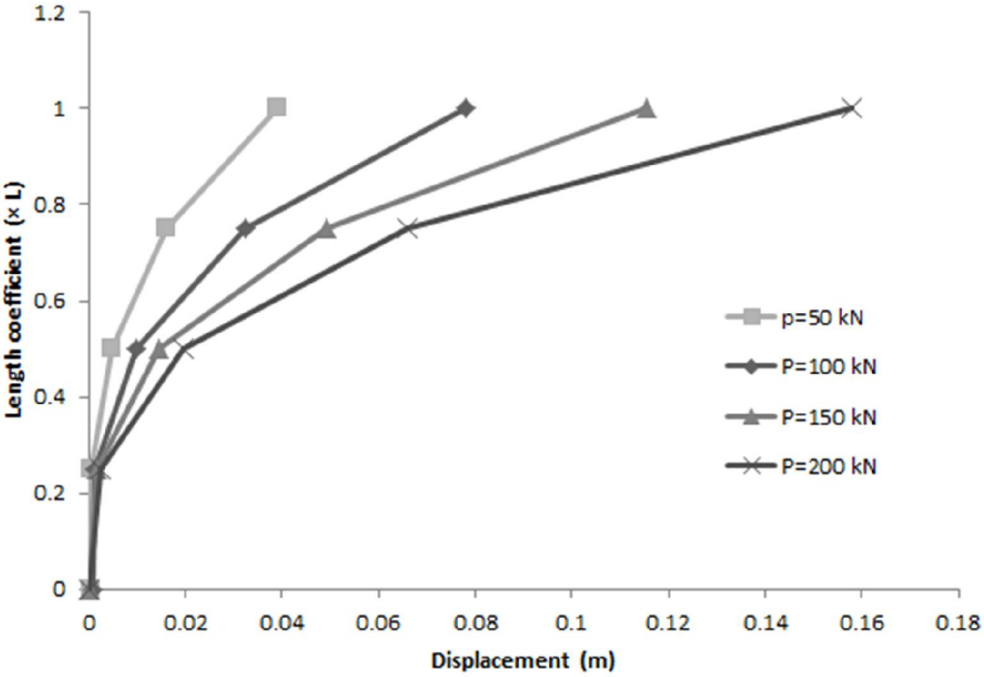

Figure 40: Lateral deflection of pile head in different depth of pile, L=5, D=0.5

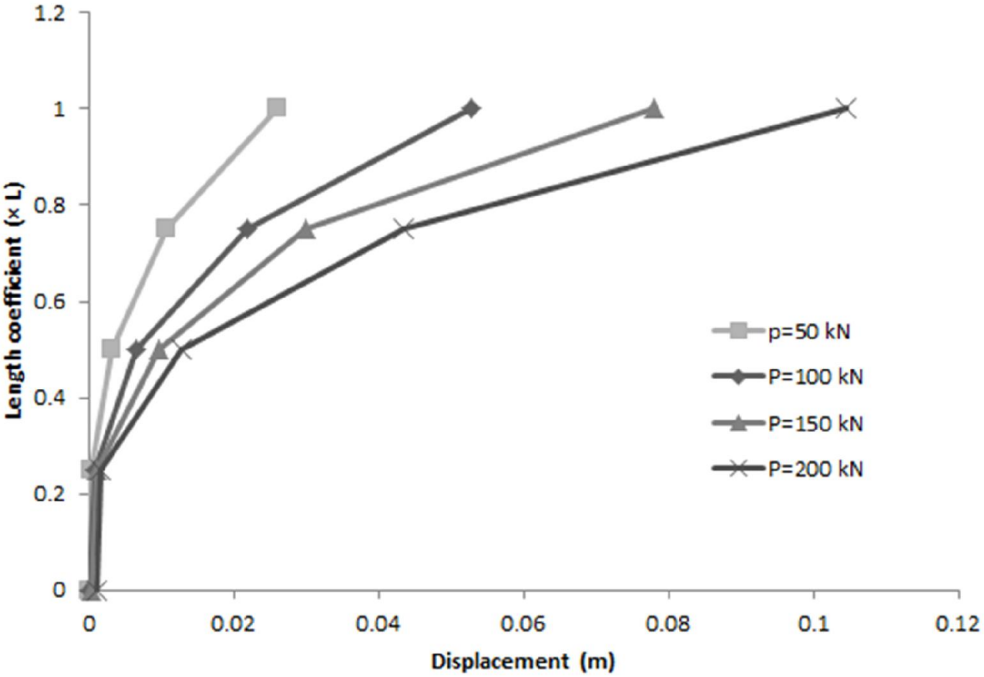

Figure 41: Lateral deflection of pile head in different depth, L=7.5, D=0.75

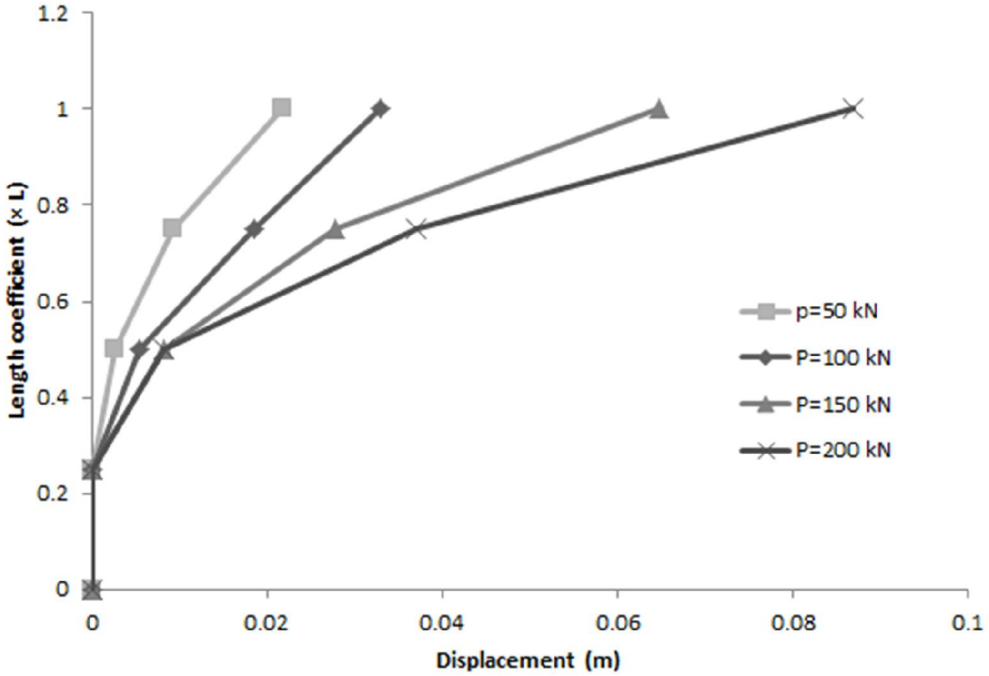

Figure 42: Lateral deflection of pile head in different depth, L=9, D=0.9

Figures 39 to 42 depict that with constant slenderness ratio under the same lateral load, increasing pile length and diameter, the lateral deflection of pile head decreases. It is because of the effect of soil mass and lateral soil pressure. It shows that the effect of lateral soil pressure and soil mass overcomes the effect of pile geometry.

Figures 43 to 46 demonstrate lateral deflection of pile with slenderness ratio of 20 at different depths along the pile shaft from the bottom (0.25L, 0.5L, 0.75L, L) under different lateral loads (50, 100, 150, 200 kN) in soil with elastic behavior.

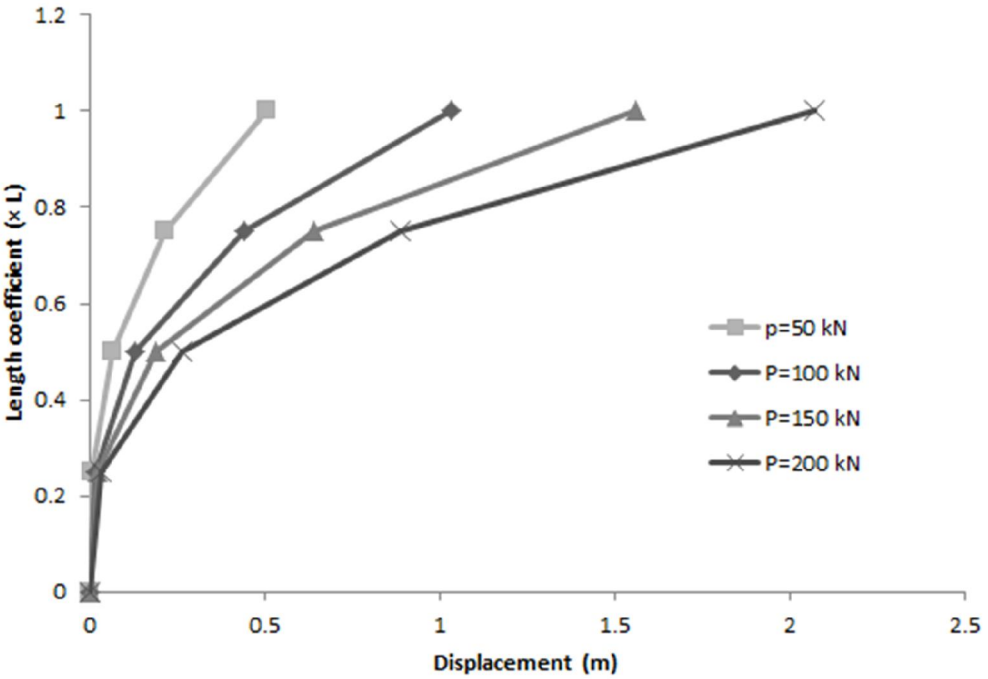

Figure 43: Lateral deflection of pile head in different depth, L=6, D=0.3

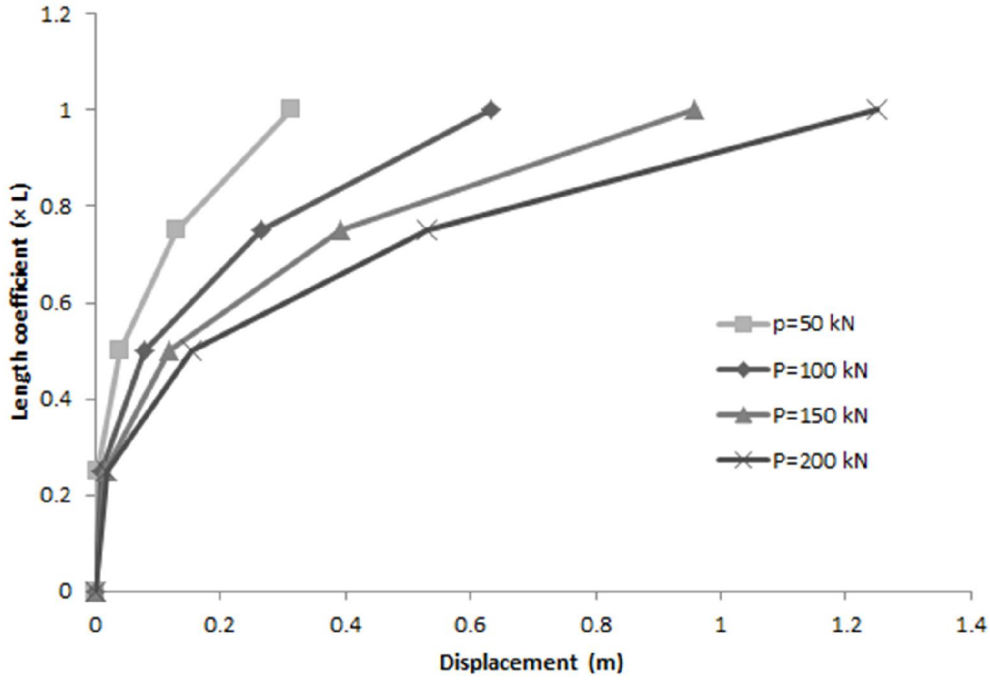

Figure 44: Lateral deflection of pile head in different depth, L=10, D=0.5

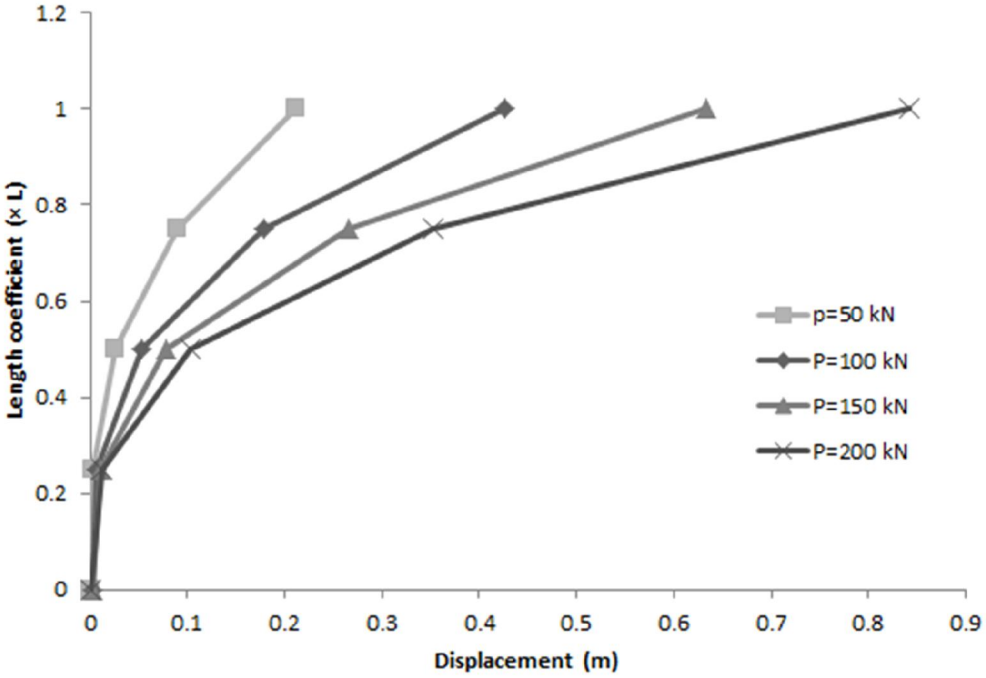

Figure 45: Lateral deflection of pile head in different depth, L=15, D=0.75

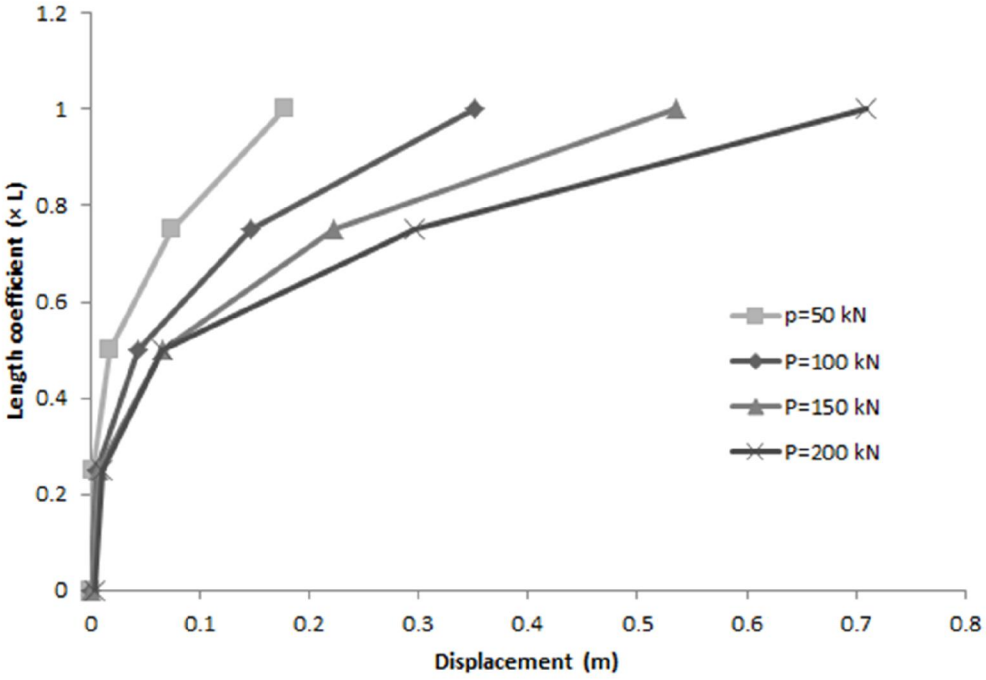

Figure 46: Lateral deflection of pile head in different depth, L=18, D=0.9

By comparing the lateral deflection of piles with L/D =20 in Figures 43 to 46 with piles with L/D =10, it can be observed that the lateral deflection in pile with higher slenderness ratio is greater than the pile with less slenderness ratio.

Figure 47 shows the comparison between maximum lateral deflection of piles with slenderness ratio of 10 which are under load P= 200 kN, and Figure 48 shows the same comparison but for slenderness ratio of 20.

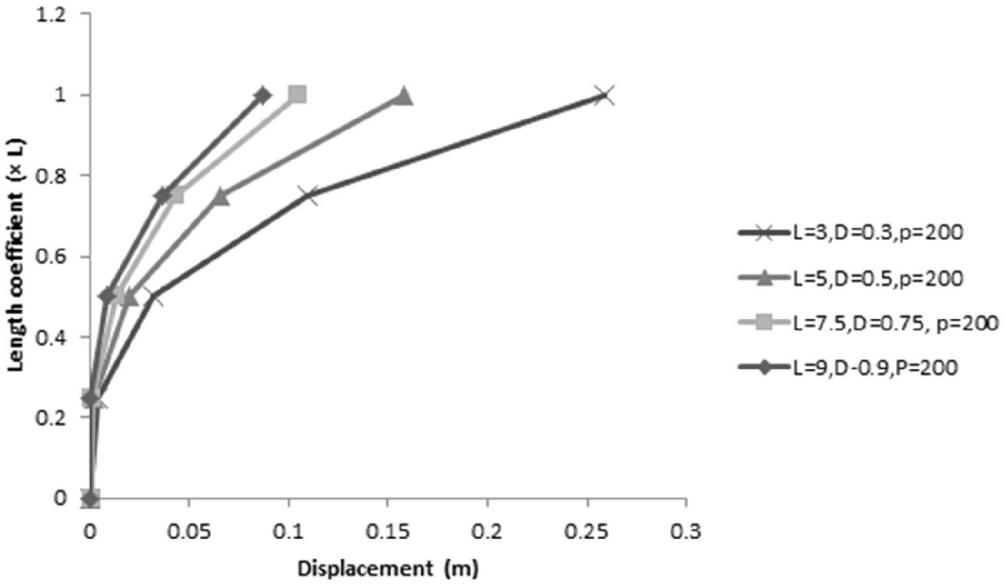

Figure 47: Comparison between max lateral deflections of pile head in different depth for (L/D) =10

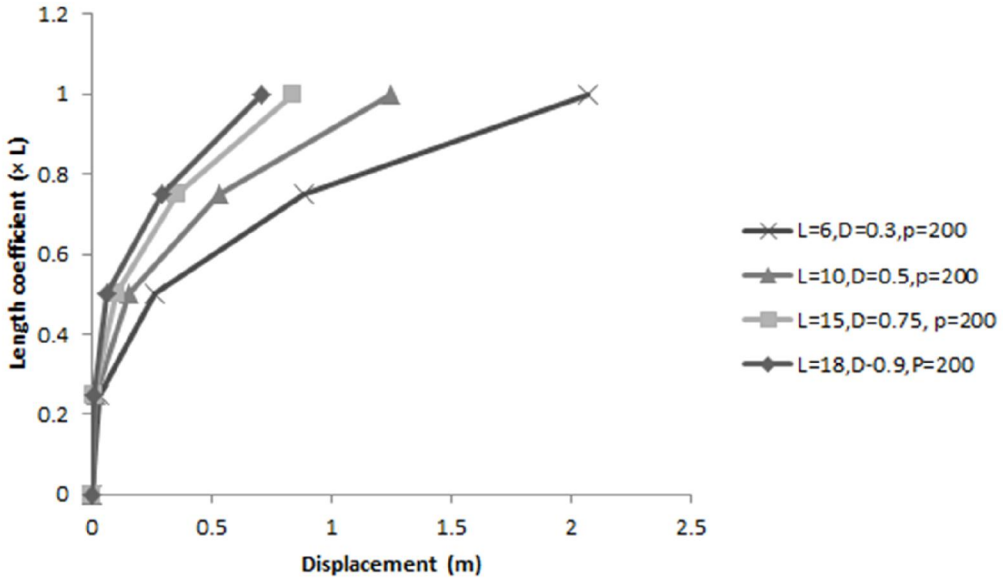

Figure 48: Comparison between max lateral deflections of pile head in different depth for (L/D) =20

Figures 47 and 48 demonstrate that under constant loading and constant slenderness ratio, the piles with higher length and bigger diameter have less lateral deflection. This can be attributed to the diameter effect which by increasing the surface area and skin friction between pile surface and soil increased.

Figure 49 shows the comparison of the lateral deflection of pile head with different slenderness ratios of 10 and 20 under different loading in soil with elastic behavior.

Figure 50 presents comparison of the lateral deflection of pile head under lateral loading with different slenderness ratios in soil with elasto-plastic behavior.

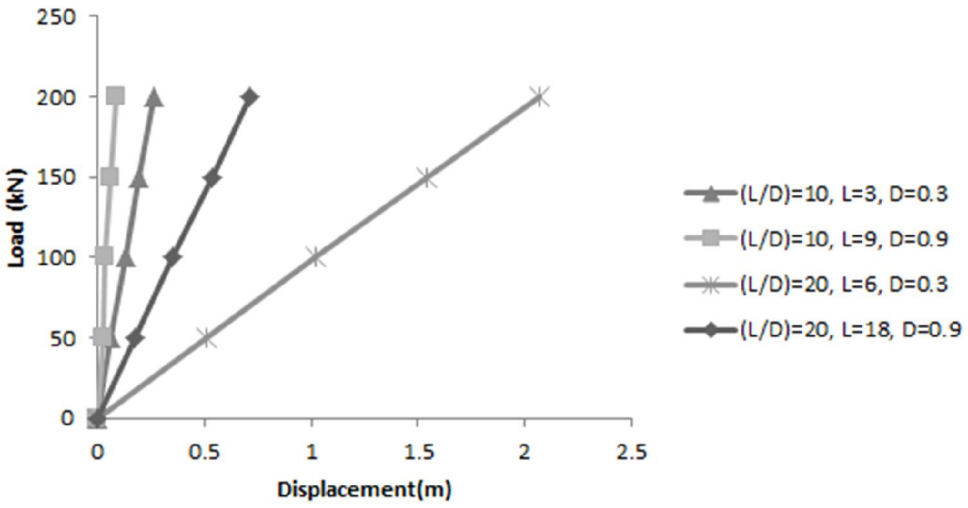

Figure 49: Pile head deflection vs. Lateral loading in plastic behavior of soil

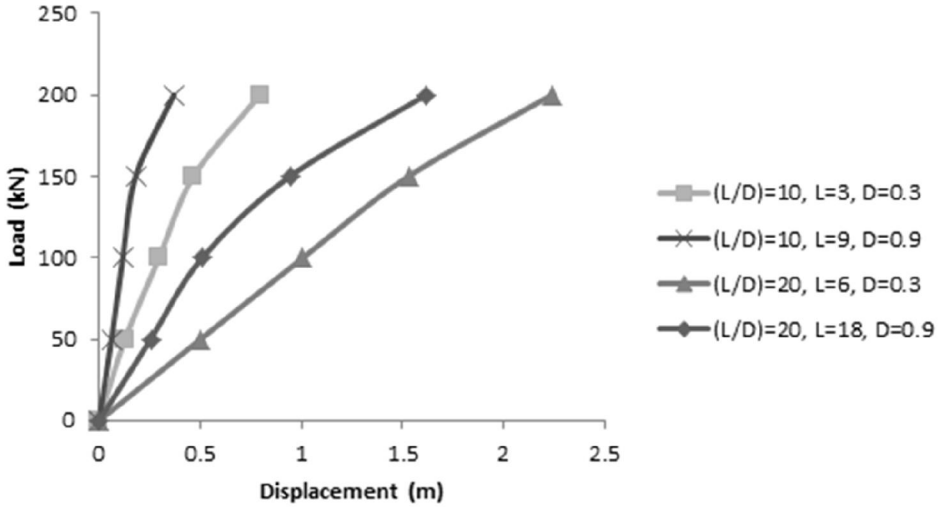

Figure 50: Lateral deflection of pile head under lateral loading in elasto-plastic behavior of soil

The comparison between lateral deflection of pile in elastic and elasto-plastic soil for pile with slenderness ratios of 10 and 20 is presented in Figures 51 and 52 respectively (D=0.9 m, L=9 m, 18 m under P=200 kN).

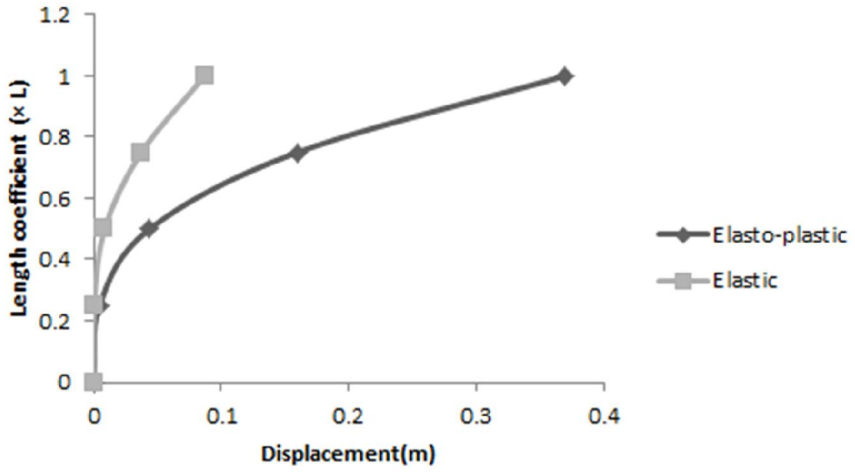

Figure 51: Comparison between Elastic and Elasto-plastic results for (L/D) =10

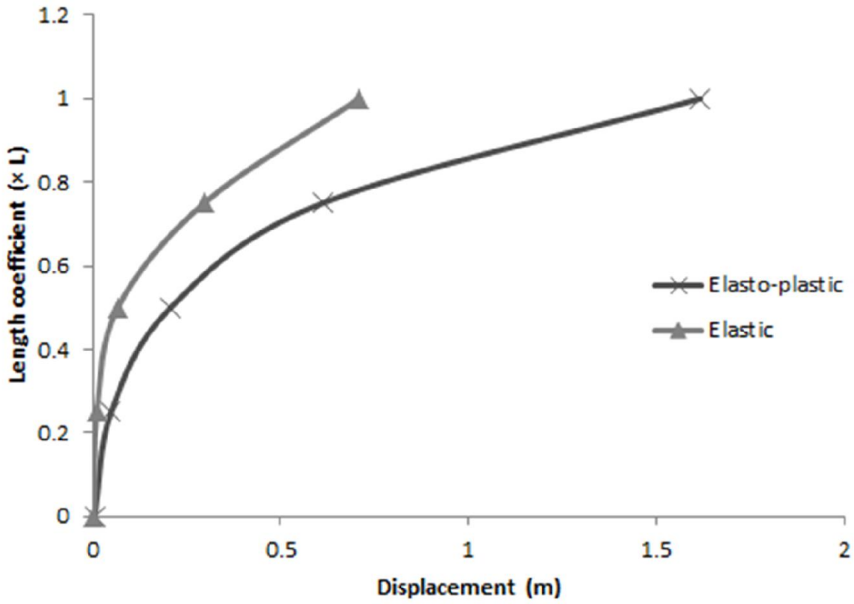

Figure 52: Comparison between Elastic and Elasto-plastic results for (L/D) =20

According to Figures 51 and 52, it can be concluded that the pile behavior in elasto-plastic soil is more critical than in elastic soil.

Figures 53 and 54 illustrate lateral deflection of pile with slenderness ratio of 10, at different depths along the pile shaft (0.25L, 0.5L, 0.75L, L) under different lateral loads (50, 100, 150, 200 kN) in soil with elasto-plastic behavior.

Figures 55 and 56 present lateral deflection of pile with slenderness ratio of 20, at different depths along the pile shaft under different lateral loads (50, 100, 150, 200 kN) in soil with elasto-plastic behavior.

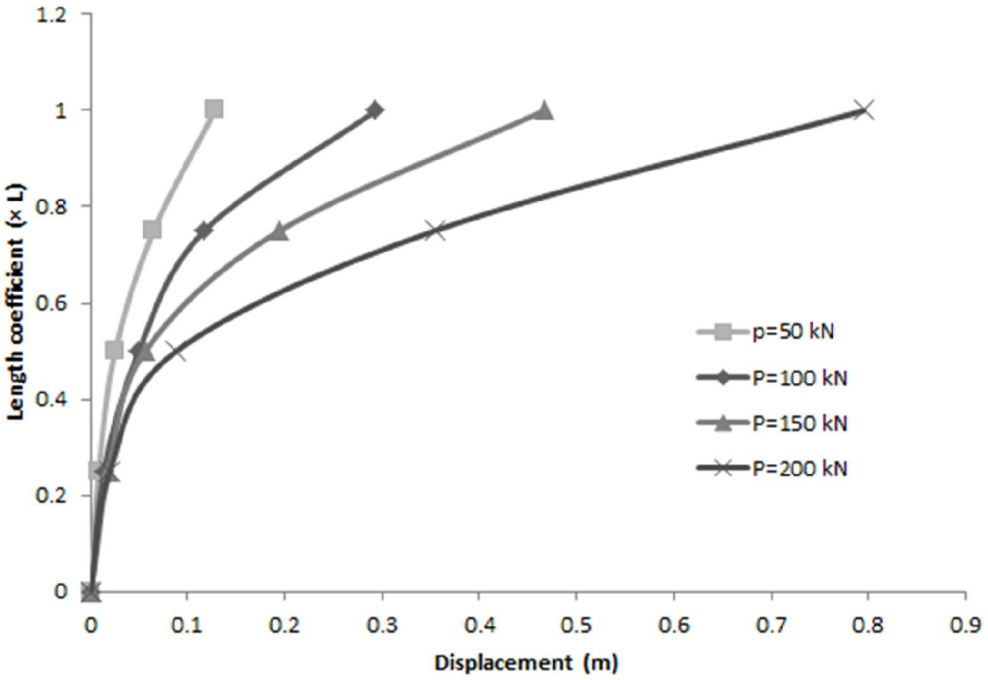

Figure 53: Lateral deflection of pile head in different depths, L=3, D=0.3

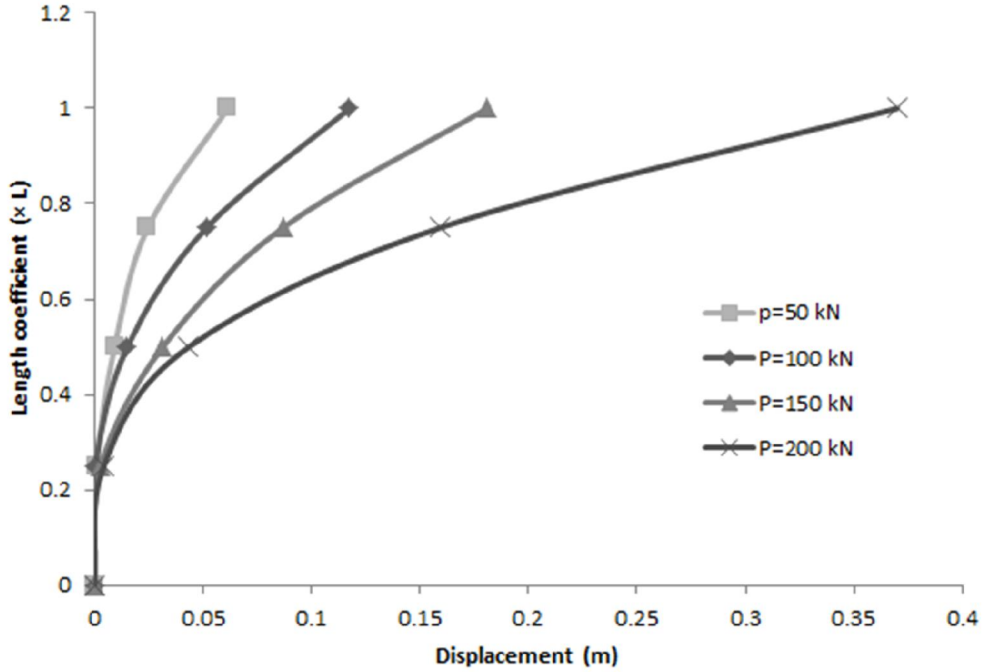

Figure 54: Lateral deflection of pile head in different depths, L=9, D=0.9

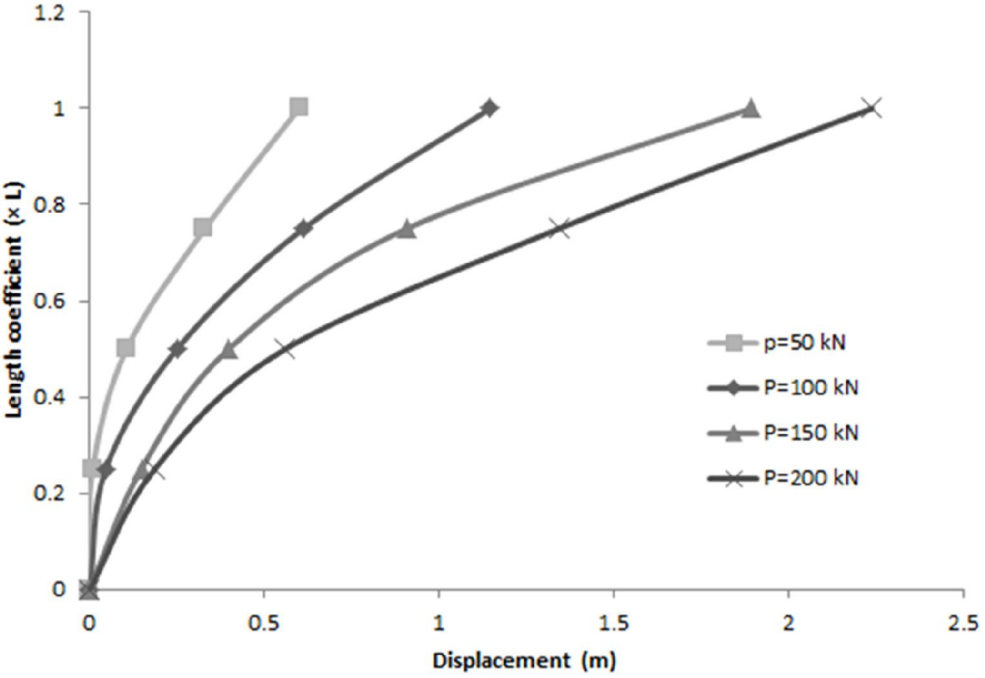

Figure 55: Lateral deflection of pile head in different depths, L=6, D=0.3

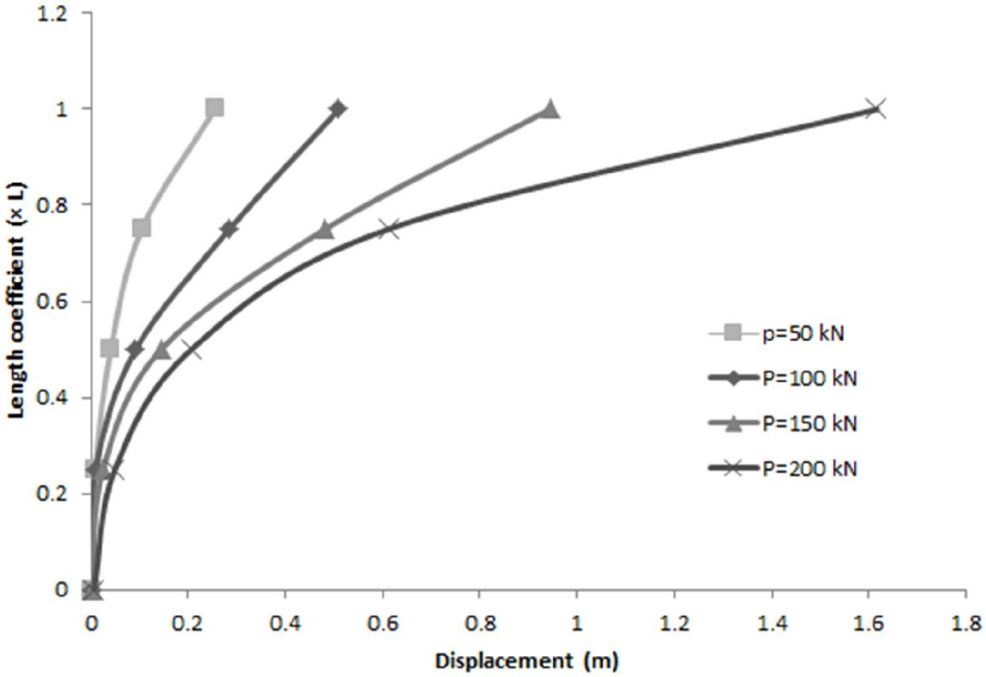

Figure 56: Lateral deflection of pile head in different depth, L=18, D=0.9

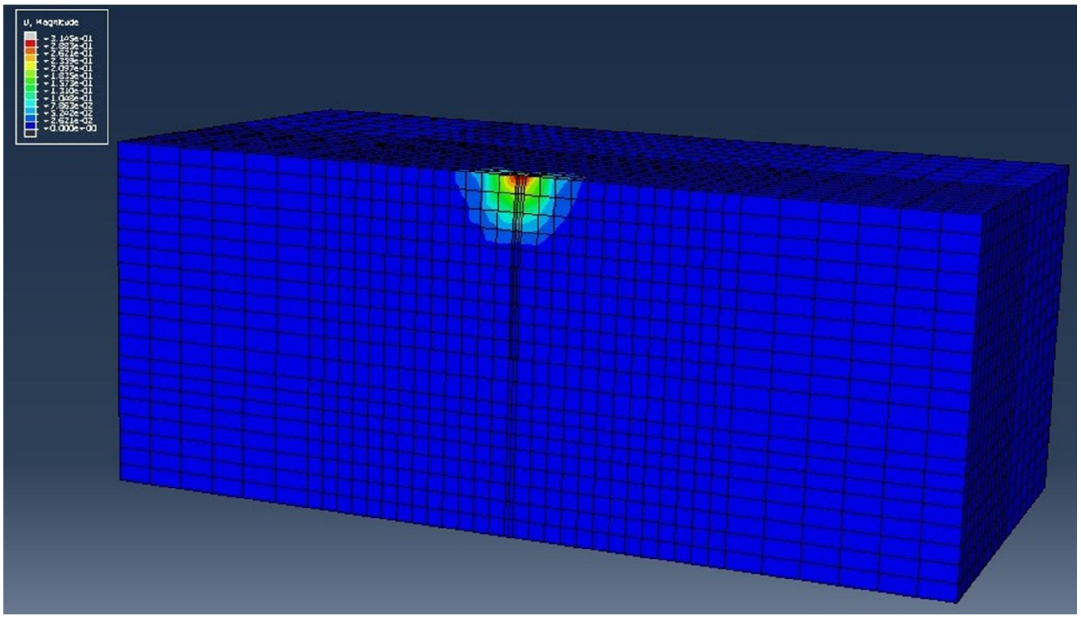

Figure 57: ABAQUS 3D plot of lateral deflection of pile under static loading for (L=10m, D=0.5m, P=50 kN)

It is obvious from Figure 57 that the most lateral deflection occurs at the pile head as shown by red color, which gets more moderate at depths along the pile length.

The normalized graphs are obtained by normalizing the depth parameter "z" with diameter "D" of the piles and plotting versus the lateral deflection of each depth along the pie shaft $\delta(z)$ with lateral deflection of pile head $\delta(0)$. These graphs shown in Figures 58 to 61 are useful for designing a pile with slenderness ratio between10 to 20 in elastic behavior of soil, by interpolation.

Similarly, Figures 62 to 65 show normalized graphs which are utilizing for pile design with $10 \leq L/D \leq 20$ in elasto-plastic behavior of soil, by interpolating a given values.

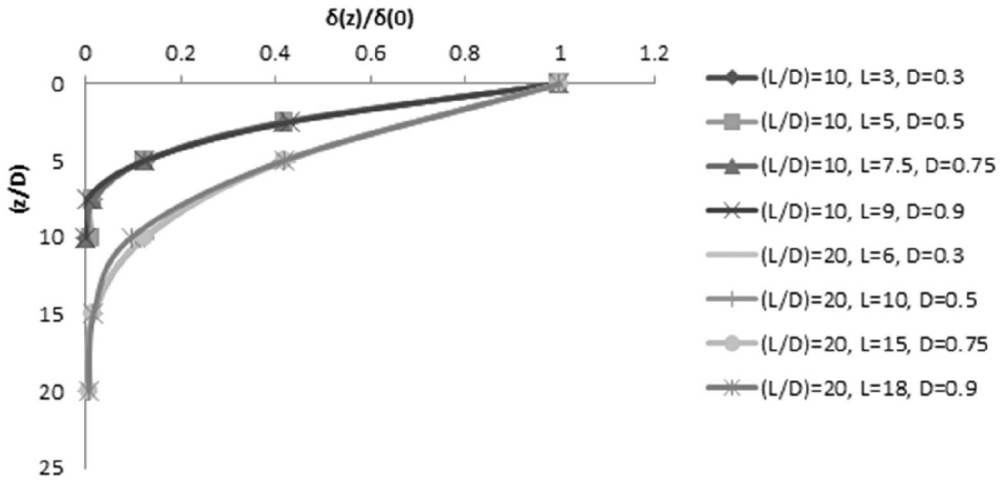

Figure 58: Pile lateral displacements along length $\delta(z)$, normal to pile head displacement along line of loading $\delta(0)$, under load P=50 kN in elastic soil

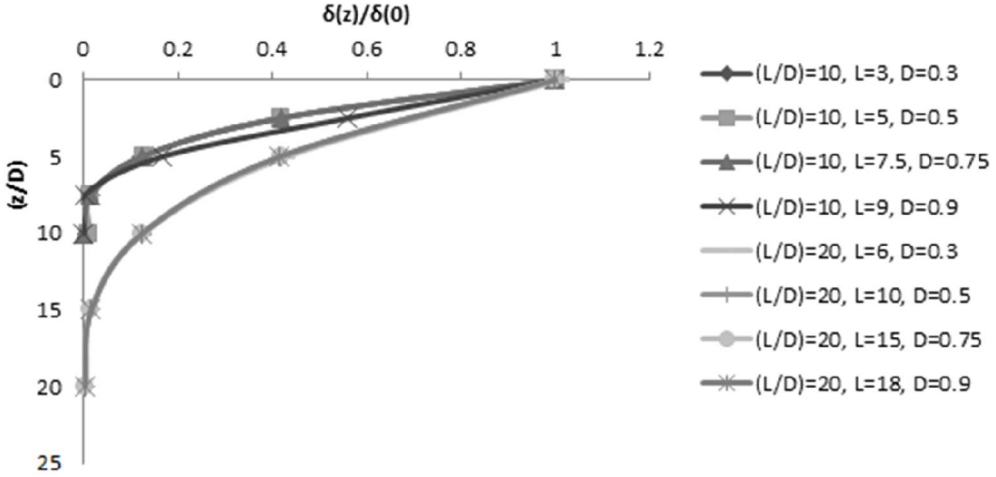

Figure 59: Pile lateral displacements along length $\delta(z)$, normal to pile head displacement along line of loading $\delta(0)$, under load P=100 kN in elastic soil

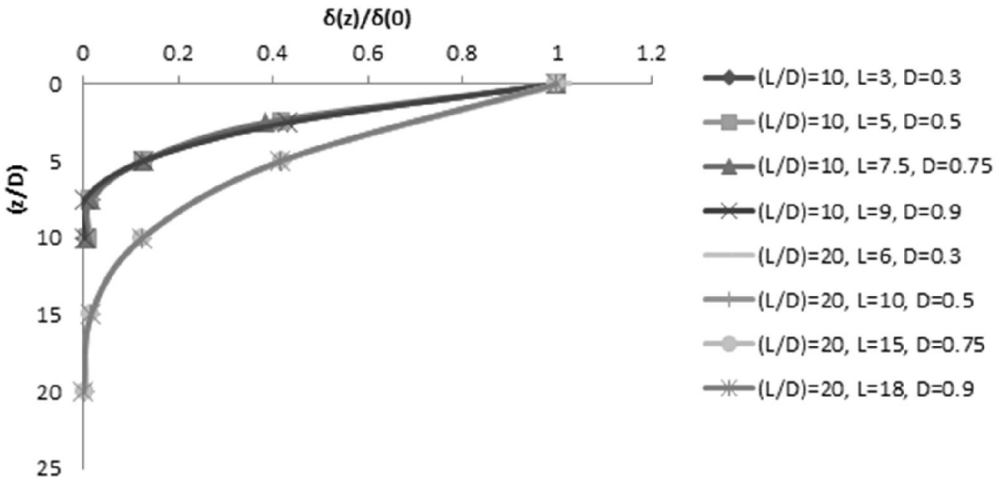

Figure 60: Pile lateral displacements along length $\delta(z)$, normal to pile head displacement along line of loading $\delta(0)$, under load P=150 kN in elastic soil

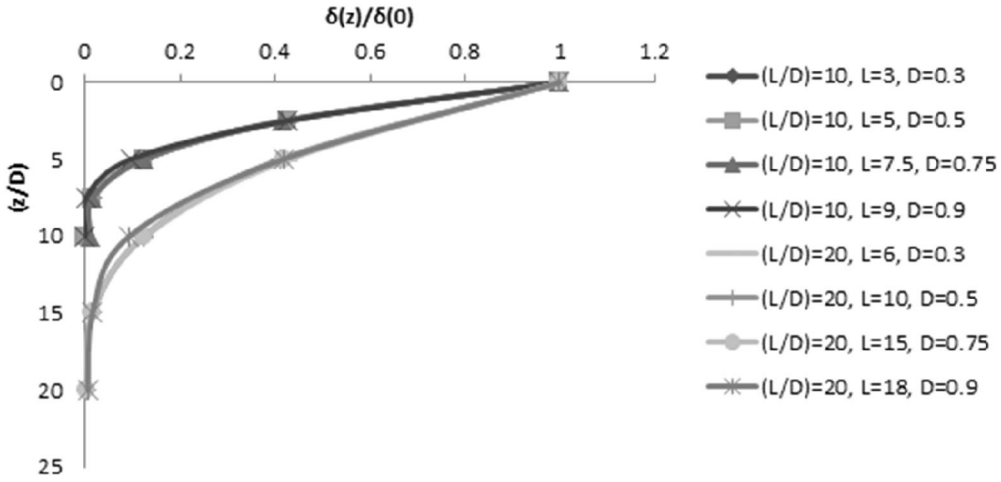

Figure 61: Pile lateral displacements along length $\delta(z)$, normal to pile head displacement along line of loading $\delta(0)$, under load P=200 kN in elastic soil

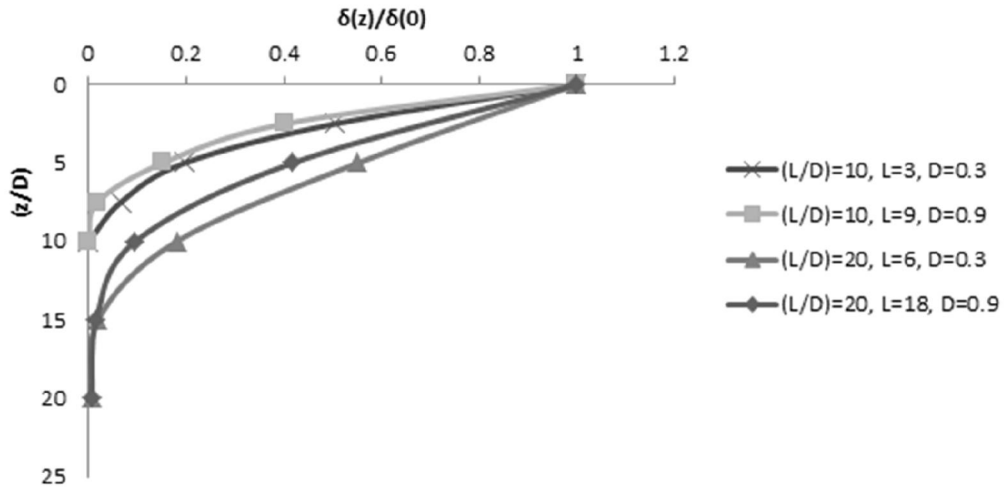

Figure 62: Pile lateral displacements along length $\delta(z)$, normal to pile head displacement along line of loading $\delta(0)$, under load P=50 kN in elasto-plastic soil

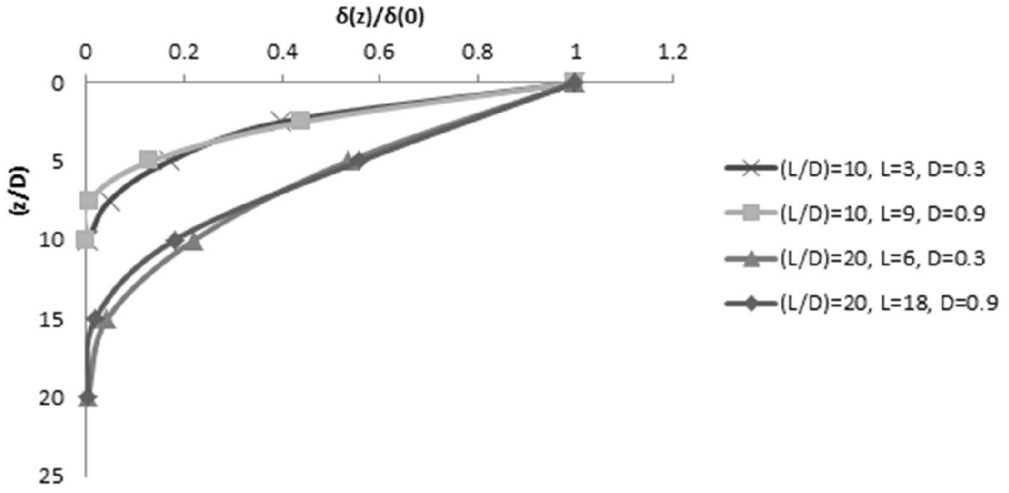

Figure 63: Pile lateral displacements along length $\delta(z)$, normal to pile head displacement along line of loading $\delta(0)$, under load P=100 kN in elasto-plastic soil

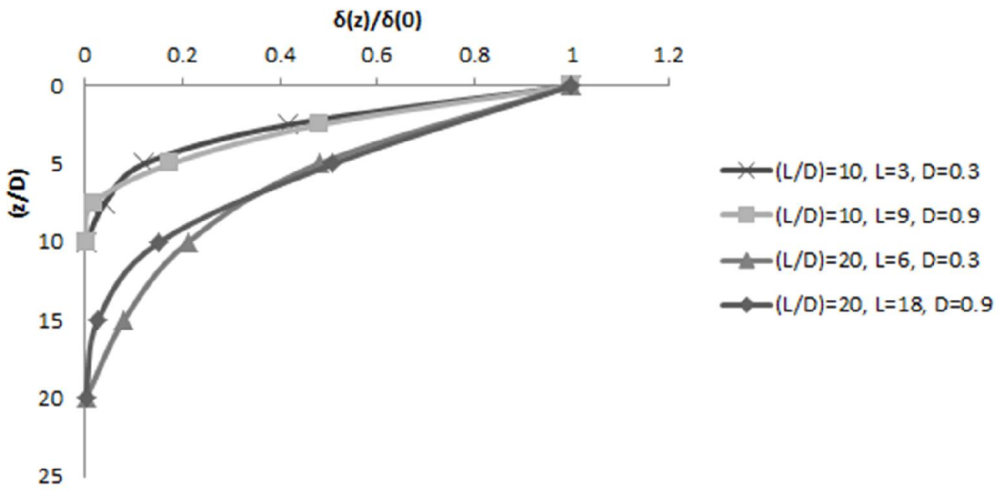

Figure 64: Pile lateral displacements along length $\delta(z)$, normal to pile head displacement along line of loading $\delta(0)$, under load P=150 kN in elasto-plastic soil

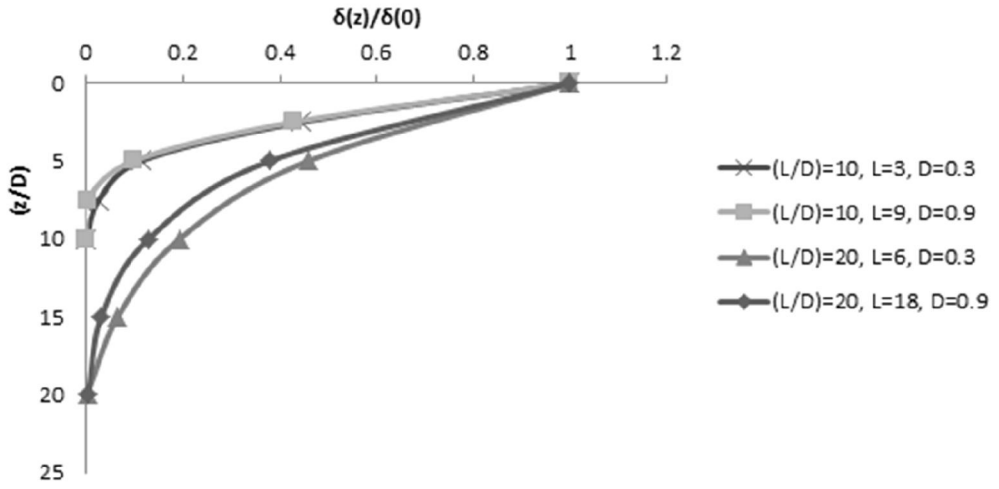

Figure 65: Pile lateral displacements along length $\delta(z)$, normal to pile head displacement along line of loading $\delta(0)$, under load P=200 kN in elasto-plastic soil

4.3 Dynamic Analysis Results in Elastic Soil

The Ricker wavelet which is described by Equation 3.8 is used to simulate a severe earthquake by substituting in the predominant frequency of Kocaeli earthquake of 1999 and the time that maximum frequency occurred. By applying this wavelet as a lateral displacement on the bedrock, and according to the wave propagation theory in homogeneous and elastic medium, it is expected that the amplitude of the SV wave which is applied on the stratum, should be double at the surface of the model, as shown in Figure 66. This figure also demonstrates the maximum displacement of the node on the middle of the soil surface as approximately 2 times of the maximum displacement of Ricker wavelet.

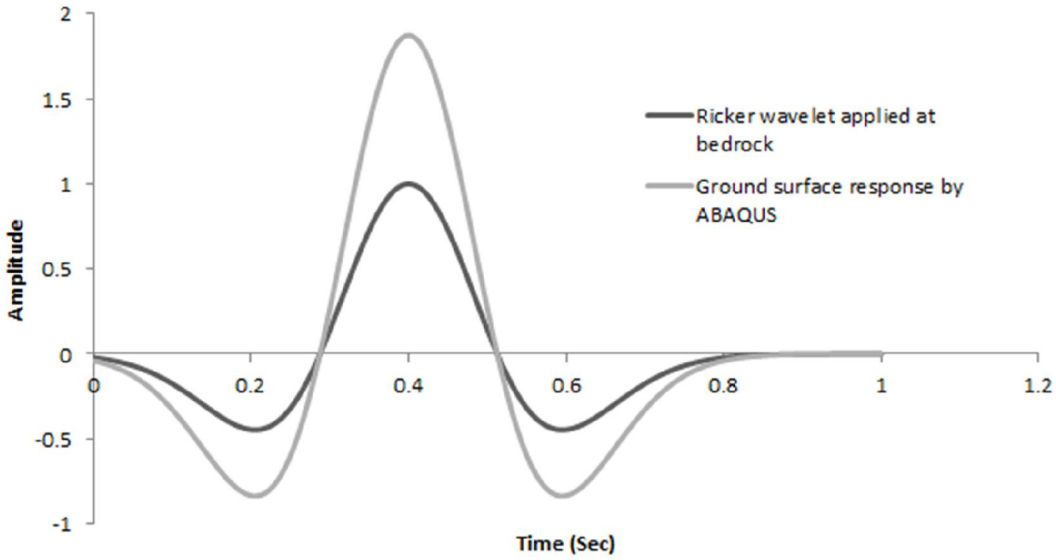

Figure 66: ABAQUS results after applied Ricker wave on the bedrock for the middle node of soil element on the surface

The ABAQUS three dimensional analysis represents this behavior in Figure 67, which shows that the critical part of free field after applying the seismic wave at the bedrock is the soil surface which is identified by red color. By moving from bedrock

to surface the incremental lateral deflection of soil under dynamic loading is revealed.

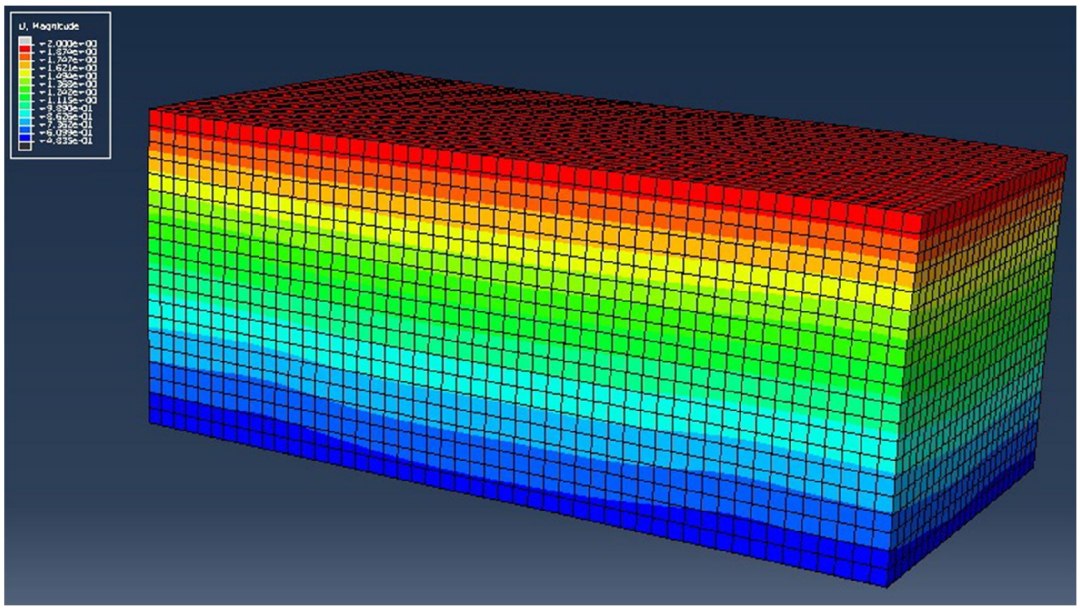

Figure 67: 3D plot of free field displacement under dynamic loading

In Figures 68 to 71 the lateral deflection of pile under wavelet excitation are presented, which indicate that lateral deflection of pile under dynamic loading is more than lateral deflection of pile under static loading of 200 kN.

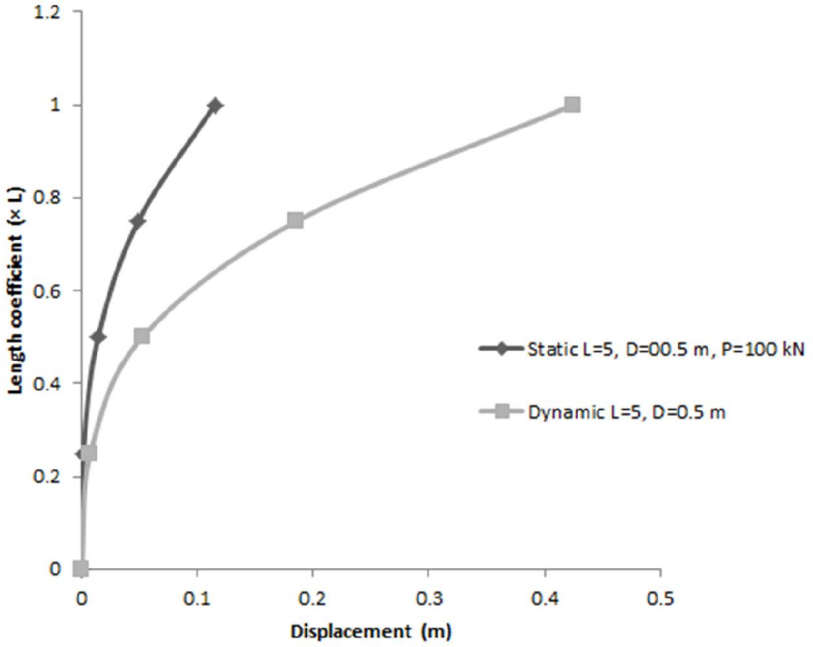

Figure 68: Comparison between lateral deflections of pile under 100kN static load and Dynamic load

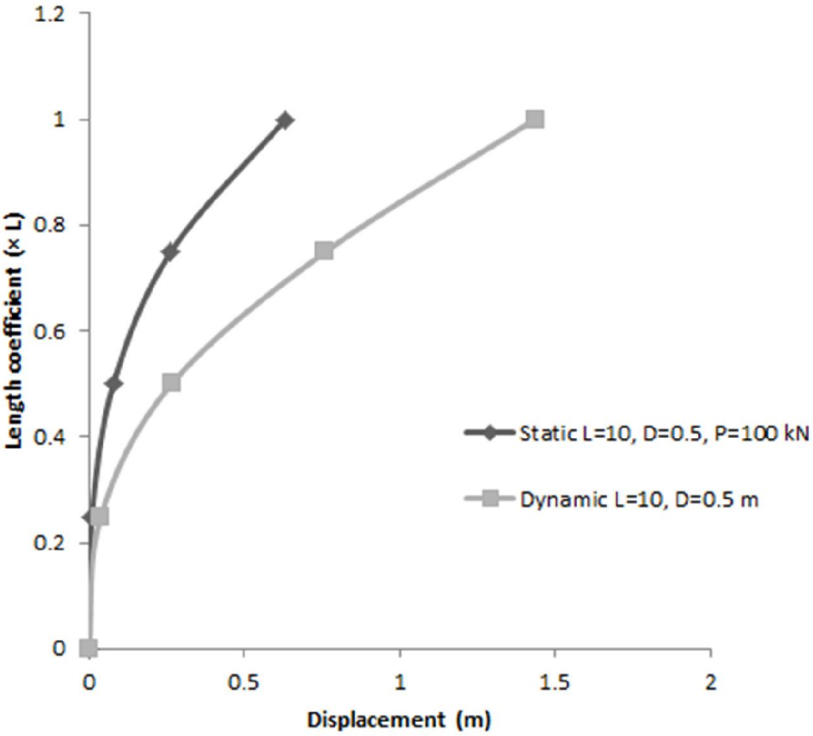

Figure 69: Comparison between lateral deflections of pile under 100kN static load and Dynamic load

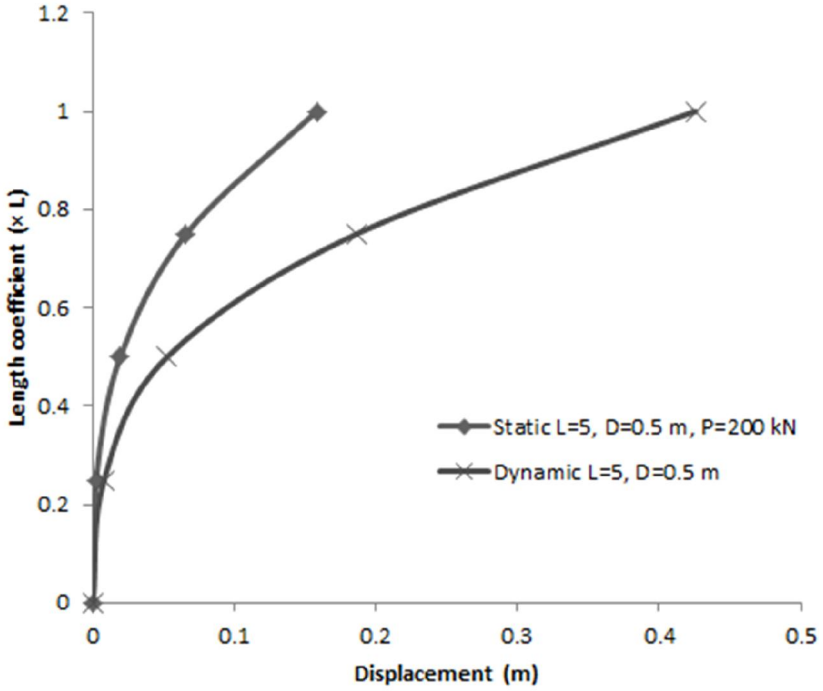

Figure 70: Comparison between lateral deflections of pile under 200 kN static load and Dynamic load

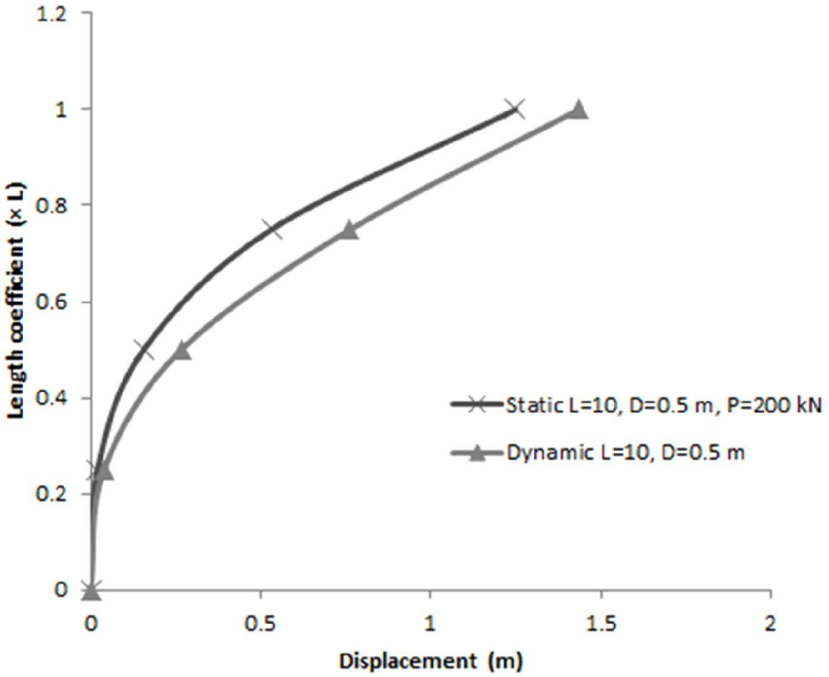

Figure 71: Comparison between lateral deflections of pile under 200 kN static load and Dynamic load

Figure 72 shows the ABAQUS three dimensional analysis for lateral deflection of pile (L / D = 10) under dynamic loading.

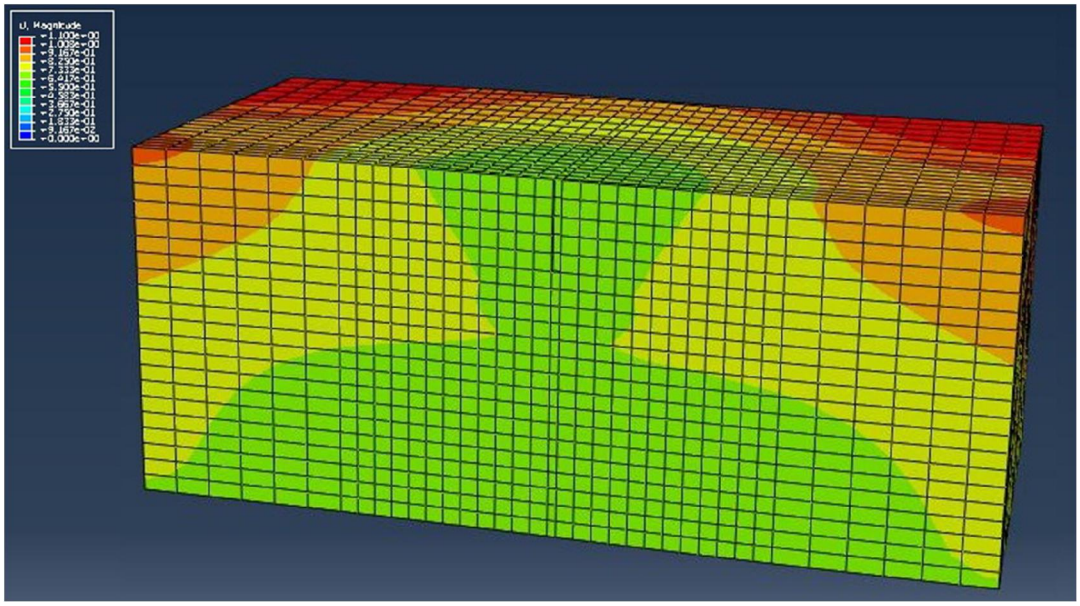

Figure 72: 3D plot of lateral deflection of pile under dynamic loading for (L=5m, D=0.5m)

It can be seen in this figure that there is less lateral displacement around the pile which is denoted by green color. However at the corner of the soil and the other side of the model, where there is no pile, the lateral deflection is higher as shown by red color.

Chapter 5

CONCLUSIONS

5.1 Conclusions

The main objective of this chapter is to illustrate the brief summary and general conclusions of the present research and recommendations for future study topics related to pile foundations.

Three dimensional finite element methods were utilized to evaluate the lateral response of elastic pile in elastic and elasto-plastic soil under lateral static and dynamic loading. The effect of slenderness ratio on lateral deflection of pile under variable static loading was assessed. For dynamic analysis the Ricker wavelet was used as a dynamic loading. The following are the main conclusions of this study.

5.1.1 Static Analysis results

The lateral response of single pile in the soil with elastic behavior by ABAQUS is too close to the beam flexural theory results.

1) In both elastic and elasto-plastic soil, by increasing the loads from 50 to 200 kN, the lateral deflection of pile was increased.

2) One of the most effective parameters on lateral deflection of pile is slenderness ratio and the pile length has more influence on increasing the lateral deflection.

3) Comparing the piles with the same slenderness ratio resulted that the piles with shorter lengths exhibited more lateral deflections. This presents the direct relation between increasing the pile fixity (lateral soil pressure) and increasing the pile length.

4) The lateral deflection of pile in elasto-plastic soil is greater than the lateral deflection of pile in elastic soil.

5.1.2 Dynamic Analysis results

1) The lateral deflection of pile in elastic soil under dynamic analysis is close to lateral pile deflection in elasto-plastic soil under static analysis.

2) It is predicted that pile deflection in elasto-plastic soil under dynamic analysis is more than pile deflection in elasto-plastic soil under static analysis.

The results of this research can be utilized in designing piles with slenderness ratios between 10 and 20.

5.2 Future Recommendations

The following topics are suggested for future studies.

1) Investigation of lateral deflection of piles in soils with different layers and properties.
2) Assessment of effect of liquefaction of soil on pile behavior.
3) Consideration of the effect of pore water pressures and degree of saturation of soil.
4) Evaluation of the effect of group pile on lateral response of piles.
5) Using real earthquake loading for dynamic analysis.

REFERENCES

ABAQUS. (2008). Abaqus Analysis User's manual. *Version 6.8*.

ABAQUS. (2010). *" Analysis User's manual, volume IV, Elements, ABAQUS 6.10."*.

Angelides, D., & Roesset, J. (1980). *"Nonlinear dynamic stiffness of piles"*. Massachusetts. : Research report R 80-13, Dept. of Civil Engineering, MIT, Cambridge.

API, A. (1991). *"Recommended Practice for Planning, Designing and Constructing Fixed Offshore Platforms,"*. Washington: API Recommended Practice 2A (RP 2A), 19 th Edn., Washington, D.C., pp.47-55.

Ashour, M., & Norris, G. (2000). "Modeling Lateral Soil-Pile Response Based on Soil-Pile Interaction". *Journal of Geotechnical and Geoenvironmental Engineering, ASCE*, Vol. 126(5), 420-428.

Ashour, M., Norris, G., & Pilling, P. (1998). "Lateral Loading of a Pile in Layered Soil Using the Strain Wedge Model". *Journal of Geotechnical and Geoenvironmental Engineering, ASCE*, Vol. 124(4), 303-315.

Badoni, D., & Makris, N. (1996). "Nonlinear Response of Single Piles under Lateral Inertial and Seismic Loads". *Soil Dynamics and Earthquake Engineering, Vol. 15*, 29-43.

Baguelin, F., Frank, R., & Saïd, Y. (1977). "Theoretical study of lateral reaction mechanism of piles". *Geotechnique 27, No. 3*, 405-434.

Baguelin, F., & Frank, R. (1979). "Theoretical Studies of Piles Using the Finite Element Method". *Proceedings of the Conf. Num. Methods in Offshore Piling, London, Institute of Civil Engineers*.

Banerjee, P., & Davies, T. (1978). "The Behavior of Axially and Laterally Loaded Single Piles Embedded in Non-Homogeneous Soils". *Géotechnique*, Vol. 28 (3).

Banerjee, P., & Davis, T. (1978). " The behavior of axially and laterally loaded single piles embedded in non-homogeneous soils". *Geotechnique ;28(3)*, 309–26.

Basile, F. (2002). "Integrated Form of Singular Mindlin's Solution". *Proceedings of the 10th ACME Conference, Swansea, Wales, UK*, 191-194.

Basile, F. (2003). "Analysis and design of pile groups", extract from "Numerical Analysis and Modelling in Geomechanics". *Spon press (eds J. W. Bull), London*, 2003, Chapter 10, 278-315.

Ben Jamma, S., & Shiojiri, H. (2000). "A Method for Three Dimensional Interaction Analysis of Pile-Soil System in Time Domain". *Transactions of the Japan Society for Computational Engineering and Science*, Paper No.20000013.

Bentley, K. J. (1999). "Lateral Response of Piles under Extreme Events". *Faculty of Graduate Studies The University of Western Ontario,London, Ontario* .

Bentley, K., & El Naggar , M. (2000). "Numerical Analysis of Kinematic Response of Single Piles". *Canadian Geotechnical Journal, Vol. 37*, 1368-1382.

Berger, E., Mahin, S., & Pyke, R. (1977). "Simplified Method for Evaluating Soil-Pile Structure Interaction Effects". *Proceedings of the 9th Offshore Technology Conference, Houston, Texas,* , 589-598.

Bhowmik, S., & Long, J. (1991). "An analytical investigation of the behavior of laterally loaded piles" . *Proc. Geotech. Eng. Congress, ASCE 2, No. 27*, 1307-1318.

Boulanger, R., Curras, C., Kutter, B., Wilson, D., & Abghari, A. (1999). ''Seismic soil-pile-structure interaction experiments and analyses.'' . *J. Geotech. and Geoenvir. Engrg. , ASCE, 125(9),* , 750–759.

Boulanger, R., Idriss, I., Hutchinson, T., & Chai, Y. (2004). "Inelastic Seismic Response of Extended Pile-Shaft-Supported Bridge Structures". *Earthquake Spectra,EERI, Vol. 20 (4),* , 1057-1080.

Bowles, J. (1974). *"Analytical and Computer Methods in Foundation Engineering"*. New York: McGraw-Hill Companies.

Bowles, J. (1996). *"Foundation Analysis and Design"*. New York: McGraw-Hill Companies.

Bransby, M. (1999). "Selection of p-y curves for piles". *Int. J. Num. Anal. Meth. Geomech. 23*, 1909-1926.

Bransby, M. F. (1999). "Selection of p-y Curves for the design of single laterally loaded piles". *International Journal for Numerical and Analytical Methods In Geomechanics*, 1909-1926.

Broms, B. (1964). "Lateral resistance of piles in cohesionless soils". *J Soil Mech Found Div – ASCE 1964;90(3)*, 56-123.

Broms, B. (1964a). " Lateral resistance of Piles in Cohesive Soils ". *Journal of the Soil Mechanics and Foundations Division, ASCE*, Vol 90(2), 27-63.

Broms, B. (1964b). " Lateral resistance of Piles in Cohesionless Soils ". *Journal of the Soil Mechanics and Foundations Division, ASCE*, Vol 90(3), 123-156.

Broms, B. (1965). " Design of Laterally Loaded Piles ". *Journal of the Soil Mechanics and Foundations Division, ASCE*, Vol 91(3), 79-99.

Brown, D., & Shie., C.-F. (1991). "Some numerical experiments with a three dimensional Finite element model of a laterally loaded pile". *Computers and Geotechnics*, 12:149-162.

Brown, D., Hidden, S., & Zhang, S. (1994). "Determination of P-Y curves using inclinometer data". *Geotech. Test. J., GTJODJ, 17, No. 2*, 150-158.

Brown, D., O'Neil, M., Hoit, M., McVay, M., El Naggar, M., & Chakraborty, S. (2001). *"Static and Dynamic Lateral Loading of Pile Groups"*. Washington, D.C: National Cooperative Highway Research Program, NCHRP Report 461, Transportation Research Board – National Research Council, National Academy Press.

Chen, W., & Liu, X. (1990). "Limit analysis in soil mechanics". *Elsevier science publishers B.V. 1990. ISBN 0-444-43042-3 (vol. 52)*.

Chen, W., & Baladi, G. (1985). "Soil plasticity, Theory and implementering ". *Elsevier science publishers B.V. ISBN 0-444-42455-5 (vol. 38)*.

Chen, W., & Mizumo, E. (1990). "Nonlinear Analysis in Soil Mechanics - Theory and Implementation." . *Amsterdam, Elsevier*.

Davis, E., & Booker, J. (1971). "The Bearing Capacity of Strip Footings from the Standpoint of Plasticity Theory". *Proc. of the 1st Australian-New Zealand Conf. on Geomechanics, Melbourne, Australia*, Vol. 1.

Desai, C., & Appel, G. (1976). "3-D Analysis of Laterally Loaded Structures". *Proceedings of the 2nd Int. Conf. Num. Methods in Geomechanics, Blacksburg, Virginia, ASCE*, Vol. 1.

Douglas, D., & Davis, E. (1964). “The Movements of Buried Footings Due to Moment and Horizontal Load and the Movement of Anchor Plates”. *Géotechnique*, Vol. 14.

Drucker, D., & Prager, W. (1952). "Soil mechanics and plastic analysis for limit design.". *Quart. Appl. Math., 10,*, 157-165.

Einav, I. (2005). "Energy and variational principles for piles in dissipative soil". *Geotechnique 55, No. 7*, 515-525.

El Naggar , M., & Novak, M. (1996). “Nonlinear Analysis for Dynamic Lateral Pile Response”. *Soil Dynamics and Earthquake Engineering, Vol. 15, Elsevier Science Limited* , 233-244.

Fan, K., Gazetas, G., Kaynia, A., & Kausel, E. (1991). "Kinematic Seismic Response of Single Piles and Pile Groups," . *Journal of Geotechnical Engineering, Vol. 117, No. 12,* , pp.1860-1879.

Faruque, M., & Desai, C. (1982). "3-D material and geometric nonlinear analysis of piles". *Proceedings of the Second International Conference on Numerical Methods in Offshore Pilling, University of Texas at Austin, Texas*, pp. 553-575.

Fleming, W., Weltman, A., Randolph, M., & Elson, W. (1992). *Piling Engineering*. New York: Blackie & Son, Glasgow and Halsted Press.

Frank, L. (1985). *"Applied Finite Element Analysis for Engineers"* . Harcourt Brace Jovanovich College Publishers, Holt, Rinehart and Winston, Inc. .

Gazetas, G., & Dobry, R. (1984a). "Horizontal Response of Piles in Layered Soils". *Journal of Geotechnical Engineering, ASCE, Vol. 110 (1)*, pp. 20-40.

Gazetas, G., & Dobry, R. (1984b). "Simple Radiation Damping Model for Piles and Footings". *Journal of Engineering Mechanics, ASCE, Vol. 110 (6)*, 937-956.

Gazetas, G., & Mylonakis, G. (1998). "Seismic soil structure interaction : new evidence and emerging issues". *Geotechnical Earthquake Engineering and Soil Dynamics, ASCE, II*, pp 1119-1174.

Geological Survey Department of Cyprus. (1896-2010). *http://www.moa.gov.cy/moa/gsd/gsd.nsf/dmlHistEarth*.

Georgiadis, M. (1983). "Development of p-y curves for layered soils". *Proc. Conf. Geotech. Pract. Offshore Engng., Am. Soc. Civ. Engrs*, 536-545.

Gireesha, N., & Muthukkumaran , K. (2011). "Study on soil structure interface strength property ". *International Journal of Earth Sciences and Engineering ISSN 0974-5904, Volume 04, No 06 SPL*, pp 89-93.

Guo, W., & Lee, F. (2001). " Load transfer approach for laterally loaded piles". *Int. J. Numer. Anal. Meth. Geomech. 25, No. 11*, 1101-1129.

Hetenyi, M. (1946). “Beams on Elastic Foundations”. *University of Michigan Press,Ann Arbor,Michigan*.

Hsiung, Y. (2003). “Theoretical Elastic-Plastic Solution for Laterally Loaded Piles”. *Journal of Geotechnical and Geoenvironmental Engineering, ASCE*, Vol 129 (6), 475-480.

Hsiung, Y., & Chen, Y. (1997). " Simplified method for analyzing laterally loaded single piles in clays" . *J. Geotech. Geoenv. Engng., Am. Soc. Civ. Engrs. 123, No. 11*, 1018-1029.

Hutchinson, T., Chai, Y., Boulanger, R., & Idriss, I. (2004). “Inelastic Seismic Response of Extended Pile-Shaft-Supported Bridge Structures”. *Earthquake Spectra,EERI*, Vol. 20 (4), 1057-1080.

Jostad, H., Andersen, K., & Tjelta, T. (1997). "Analyses of skirted foundations and anchors in sand subjected to cyclic loading". *Proc., Int. Conf. on Behavior of Offshore Structures, Vol. 1,* , 149–162.

Kagawa , T., & Kraft, L. (1980). “Lateral Load-Deflection Relationship of Piles Subjected to Dynamic Loadings”. *Soil and Foundation, Japanese Society of Soil Mechanics and Foundation Engineering, Vol. 20(4)*, 19-35.

Kagawa, T. (1992). “Modeling Soil Reaction to Laterally Loaded Piles”. *Transportation Research Record No 1336 – Foundations Engineering:*

Seismic Design, Drilled Shafts and other Issues, Transportation Research Board, Washington, 81-89.

Kagawa, T., & Kraft, L. (1981). "Lateral Piles Response During Earthquakes". *Journal of the Geotechnical Engineering Division, ASCE, Vol. 107 (12),* , 1713-1731.

Kim, B., Kim, N., Lee, W., & Kim, Y. (2004). "Experimental Load-Transfer Curves of Laterally Loaded Piles in Nak-Dong River Sand". *Journal of Geotechnical and Geoenvironmental Engineering, ASCE*, Vol. 130 (4), 416-425.

Klar, A. (2003). *"Model Studies of Seismic Behavior of Piles in Sand"*. Israel : Research Thesis, Israel Institute of Technology.

Kooijman, A., & Vermeer, P. (1988). "Elastoplastic analysis of laterally loaded piles". *Proc. 6th Int. Conf. Num. Meth.Geomech., Innsbruck, Vol. 2*, 1033-1042.

Kramer, S. (1996). *"Geotechnical Earthquake Engineering,"* . Prentice-Hall: Newjersey.

Lee, C., & Small, J. (1991). "Finite layer analysis of laterally loaded piles in cross anisotropic soils". *Int. J. Numer. Anal. Meth. Geomech. 15*, 785-808.

Lee, S., Kog, Y., & Karunaratne, G. (1987). "Laterally loaded piles in layered soil.". *Soils Fdns. 27, No. 4*, 1-10.

Maheshwari, B., Truman, K., El Naggar, M., & Gould, P. (2004). “Three-Dimensional Finite Element Nonlinear Dynamic Analysis of Pile Groups for Lateral Transient and Seismic Excitations”. *Canadian Geotechnical Journal, Vol. 41*, 118-133.

Maluis, N., & Gazetas, G. (1992). "Dynamic Pile-Soil-Pile Interaction. Part II: Lateral and Seismic Response," . *Earthquake Engineering and Structural Dynamics, Vol. 2 1* , pp.145-162. .

Matlock, H. (1970). “Correlations for Design of Laterally Loaded Piles in Soft Clay”. *Proceedings of the 2nd Offshore Tech. Conference, Houston, Texas*, Vol. 1.

Matlock, H., & Reese, L. (1960). “Generalized Solutions for Laterally Loaded Piles”. *Journal of the Soil Mechanics and Foundations Division, ASCE*, Vol. 86 (5), 63-91.

Matlock, H., Foo, S., & Bryant, L. (1978). “Simulation of Lateral Pile Behavior”. *Proceedeings of the Earthquake Engineering and Soil Dynamics Div., ASCE*.

Mostafa, Y., & El Naggar, M. (2002). “Dynamic Analysis of Laterally Loaded Pile Groups in Sans and Clay”. *Canadian Geotechnical Journal, Vol 39*, 1358-1383.

Nag Rao, K. (2006). "Numerical Modelling And Analysis of Pile Supported Embankment". *The University of Texas at Arlington*, 76.

Ng, C., & Zhang, L. M. (2001). “Three-Dimensional Analysis of Performance of Laterally Loaded Sleeved Piles in Sloping Ground”. *Journal of Geotechnical and Geoenvironmental Engineering*, Vol. 127 (6), 499-509.

Nogami, T., & Konagai, K. (1988). “Time Domain Flexural Response of Dynamically Loaded Single Piles”. *Journal of Engineering Mechanics, ASCE, Vol. 144(9)*, 1512-1525.

Nogami, T., & Novak, M. (1980). “Coefficients of Soil Reaction to Pile Vibration”. *Journal of Geotechnical Engineering, ASCE, Vol. 106(5),* , 565-570.

Novak, M. (1974). “Dynamic Stiffness and Damping of Piles”. *Canadian Geotechnical Journal, Vol 11, NRC Research Press,* , 574-598.

Novak, M., Nogami, T., & Aboul-Ella, F. (1978). “Dynamic Soil Reaction for Plane Strain Case”, . *Journal Engineering Mechanics, ASCE Vol. 104(4),*, 953-595.

Ochoa, A. (2003). Estructuras de Vigas Sobre Suelos Elásticos de Rigidez. *Revista Internacional de Desastres Naturales, Accidentes e Infraestructura, 3(2)*, 157-174.

O'Neill , M., & Murchison , J. (1983). "An evaluation of p–y relationships in sands". *Research Report No. GT-DF02-83, Department of Civil Engineering, University of Houston*.

Palmer, L., & Thompson, J. (1948). “The Earth Pressure and Deflection Along Embedded Lengths of Piles Subjected to Lateral Thrusts”. *Proceedings of the 2nd International Conference in Soil Mechanics and F.E.*, Rotterdam, Vol. 5.

.

Parmele, R., Penzien, J., Scheffey, C., Seed, H., & Thiers, G. (1964). “Seismic effects on structures supported on piles extending through dee p sensitive clays” . *Inst. Eng. Res., University of California, Berkeley, Rep. SEM* , 642.

PoLam, I., Kapuskar, M., & Chaudhuri, D. (1998). *“Modeling of Pile Footings and Drilled Shafts for Seismic Design”.* Buffalo: Technical Report MCEER-98-0018. Multidisciplinary Center for Earthquake Engineering Research, State University of New York at Buffalo.

Poorooshasb, H., Holubec , I., & Sherbourne, A. (1967). "Yielding and flow of sand in triaxial compresion". *Can Geotech. J. 4, 4*, 376-397.

Poulos , H. (1971). “Behavior of Laterally Loaded Piles: I – Single Piles”. *Journal of the Soil Mechanics and Foundation Division, ASCE*, Vol. 97 (SM5), 711-731.

Poulos, H. (1972). “Behavior of Laterally Loaded Piles: III – Socketed Piles”. *Journal of the Soil Mechanics and Foundation Division, ASCE*, Vol 98 (SM4), 733-751.

Poulos, H. G., & Davis, E. H. (1980). *"Pile Foundation Analysis and Design"*. Newyork: John Wiley and sons.

Poulos, H., & Davis, E. (1974). *"Elastic Solutions for Soil and Rock Mechanics"*. New York: John Wiley & Sons.

Prakash , S., & Sharma, H. (1990). *" Pile Foundations in Engineering Practice"*. Canada: John wiley & Sons.

Pyke, R., & Beikae, M. (1984). "A new solution for for the resistance of single piles to lateral loading". *Laterally Loaded Deep Fdns., ASTM STP 835*, 3-20.

Randolph, M. (1981). "The response of flexible piles to lateral loading". *Géotechnique 31, No. 2*, 247-259.

Reese, L. (1977). "Laterally Loaded Piles: Program Documentation". *Journal of the Geotechnical Engineering Division, ASCE*, Vol 103.

Reese, L., & Matlock, H. (1956). "Non-Dimensional Solutions for Laterally Loaded Piles with Soil Modulus Assumed Proportional to Depth". *Proc. 8th Texas Conf. S.M. and F.E.*, Spec. Pub. 29, Bureau of Eng. Res., Univ. of Texas, Austin. .

Reese, L., & Van Impe, W. (2001). *" Single Piles and Pile Groups Under Lateral Loading"*. London UK: Taylor & Francis Group plc.

Reese, L., & Welch, R. (1975). "Lateral loading of deep foundations in stiff clay". *J.Geotech. Engng. Div., Am. Soc. Civ. Engrs. 101, No. GT7*, 633-649.

Reese, L., Cox, W., & Koop, F. (1974). "Analysis of laterally loaded piles in sand". *Proc. 6th Offshore Tech. Conf., Houston, Texas, 2*, 473-483.

Ricker, N. (1960). "The form and laws of propagation of seismic wavelets." . *Geophysics 18*, pp. 10-40.

Scott, R. (1981). *"Foundation Analysis"*. Englewood Cliffs, NJ: Prentice-Hall.

Serdaroglu, M. (2010). "Nonlinear analysis of pile driving and ground vibrations in saturated cohesive soils using the finite element method.". *Doctor of Philosophy degree in Civil and Environmental Engineering ,University of Iowa*.

Shahrour, I., Ousta, R., & Sadek, M. (2001). "Seismic behavior of micropiles used as foundation support elements." . *Transportation Research Record 1772*, pp. 84-90.

Shen, W., & Teh, C. (2004). "Analysis of Laterally Loaded Piles in Soil with Stiffness Increasing with Depth". *Journal of Geotechnical and Geoenvironmental Engineering, ASCE* , Vol 130 (8), 878-882.

Sogge, R. (1981). " Laterally loaded pile design". *J. Geotech. Engng. Div., Am. Soc. Civ. Engrs 107, No. GT9*, 1179-1199.

Spillers, W., & Stoll, R. (1964). “Lateral Response of Piles”. *Journal of the Soil Mechanics and Foundation Division, ASCE*, Vol. 90 (6), 1-9.

Sun, K. (1994). "Laterally loaded piles in elastic media". *J. Geotech. Engng., Am. Soc. Civ. Engrs. 120, No. 8*, 1324-1344.

Tajimi, H. (1966). *"Earthquake response of Foundation Structures (in Japanese) Report.* Tokyo: Faculty of Science and Engineering, Nihon University Tokyo 1.1-3.5.

Thomas, L., Aykut , A., & US Geology Surveying Department . (November 1999). *"Implications for Earthquake risk reduction in the United state from the Kocaeli,Turkey earthquake of August 17, 1999 ".* Colorado: in the Central Region, Denver.

Tomlinson, M., & Woodward, J. (2008). *" Pile Design and Construction Practice".* Newyork: Taylor & Francis.

Trochanis, A., Bielak, J., & Christiano, P. (1988). *"A Three-Dimensional Nonlinear Study of Piles Leading to the Development of a Simplified Model," A Technical Report of Research Sponsored by The NSF, Grant No. ECE-86/1060, Carnegie Mellon* . NSF, Grant No. ECE-86/1060, Carnegie Mellon University.

Trochanis, A., Bielak, J., & Christiano, P. (1991). "Simplified model for analysis of one or two piles". *Journal of Geotechnical Engineering , ASCE, Vol. 117, No. 3*, pp. 448-466.

Vesic, A. (1961). "Bending of Beams Resting on Isotropic Elastic Solid". *Journal of the Engineering Mechanics Division, ASCE*, Vol 87 (2), 35-53.

Vlasov, V., & Leont'ev, N. (1966). " Beams, plates and shells on elastic foundations". *Israel Program for Scientific Translations, Jerusalem*.

Wang , S., Kutter, B., Chacko, M., Wilson, D., Boulanger, R., & Abghari, A. (1998). "Nonlinear Soil-Pile Structure Interaction". *Earthquake Spectra, EERI*, Vol. 14(2), 377-396.

Wolf, J. (1985). *"Dynamic Soil-Structure Interaction"*. NJ: Prentice-Hall, Englewood Cliffs.

Wu, G., & Finn, W. (1996). "Dynamic Nonlinear Analysis of Pile Foundations Using Finite Element Method in the Time Domain,". *Canadian Geotechnical Journal, Vol. 34*, pp.44-52.

Wu, G., & Finn, W. (1997). "Dynamic nonlinear analysis of pile foundations using finite element method in the time domain". *Canadian Geotechnical Journal, 34*, 44–52.

Yang, Z., & Jeremic, B. (2002). “Numerical Analysis of Pile Behavior under Lateral Loads in Layered Elastic-Plastic Soils”. *International Journal for Numerical and Analytical Methods in Geomechanics*, Vol 26, 1385–1406.

Zienkiewicz, O., & Cheung, Y. (1967). *"The Finite Element Method in Continuum and Structural Mechanics"*. Newyork: McGraw-Hill Book Company; First Edition edition 272 pp.